OULU 2011
C 389

ACTA

UNIVERSITATIS OULUENSIS


*Jan Nissinen*

# INTEGRATED CMOS CIRCUITS FOR LASER RADAR TRANSCEIVERS

*UNIVERSITY OF OULU,*
*FACULTY OF TECHNOLOGY,*
*DEPARTMENT OF ELECTRICAL ENGINEERING;*
*UNIVERSITY OF OULU,*
*INFOTECH OULU*

ACTA UNIVERSITATIS OULUENSIS
C Technica 389

*JAN NISSINEN*

# INTEGRATED CMOS CIRCUITS FOR LASER RADAR TRANSCEIVERS

Academic dissertation to be presented with the assent of the Faculty of Technology of the University of Oulu for public defence in OP-sali (Auditorium L10), Linnanmaa, on 3 November 2011, at 12 noon

UNIVERSITY OF OULU, OULU 2011

Acta Univ. Oul. C 389, 2011

Supervised by
Professor Juha Kostamovaara

Reviewed by
Professor Torben Larsen
Docent Sven Mattisson

ISBN 978-951-42-9544-7 (Paperback)
ISBN 978-951-42-9545-4 (PDF)

ISSN 0355-3213 (Printed)
ISSN 1796-2226 (Online)

Cover Design
Raimo Ahonen

JUVENES PRINT
TAMPERE 2011

**Nissinen, Jan, Integrated CMOS circuits for laser radar transceivers.**
University of Oulu, Faculty of Technology, Department of Electrical Engineering, Infotech Oulu, P.O. Box 4500, FI-90014 University of Oulu, Finland
*Acta Univ. Oul. C 389, 2011*
Oulu, Finland

***Abstract***

The main aim of this work was to design CMOS receiver channels for the integrated receiver chip of a pulsed time-of-flight (TOF) laser rangefinder. The chip includes both the receiver channel and the time-to-digital converter (TDC) in a single die, thus increasing the level of integration of the system, with the corresponding advantages of a cheaper price and lower power consumption, for example.

Receiver channels with both linear and leading edge timing discriminator schemes were investigated. In general the receiver channel consists of a preamplifier, a postamplifier and a timing comparator. Since a large systematic timing error may occur due to high variation in the amplitude of the received echo, a leading edge timing discriminator scheme with time domain walk error compensation is proposed here, making use of the TDC already available in the chip to measure the slew rate of the pulse and using that information to evaluate the timing error. This compensation scheme benefits from the fact that compensation can be continued even though the signal is clipped in the amplitude domain, because the slew rate continues to increase even then.

The receiver channel with leading edge detection and time domain walk error compensation achieved a compensated timing walk error of ±4.5 mm within a dynamic range of more than 1:10000. The standard deviation in single shot precision was less than 25 mm with an SNR of more than 20. The usability of the receiver channel in pulsed TOF laser rangefinders was verified by making actual time-of-flight measurements on a calibrated measurement track. The linearity of the receiver chip was better than ±5 mm in a measurement range from 3 m to 21 m, with the dynamic range of the receiver channel reaching more than 1:2000.

An integrated CMOS laser diode pulser was also demonstrated to prove its functionality for generating ampere-scale peak current pulses through a low ohmic load and a laser diode. The CMOS pulser achieved a peak current pulse with the amplitude of ~1 A, an optical pulse width of ~2.5 ns and a rise time of ~1 ns with a 5 V power supply.

*Keywords:* distance measurement, integrated CMOS receiver channel, laser pulser, timing discrimination

**Nissinen, Jan, Integroituja CMOS-piirejä lasertutkan lähetin-vastaanottimiin.**
Oulun yliopisto, Teknillinen tiedekunta, Sähkötekniikan osasto, Infotech Oulu, PL 4500, 90014 Oulun yliopisto
*Acta Univ. Oul. C 389, 2011*
Oulu

### *Tiivistelmä*

Työn ensisijaisena tavoitteena oli suunnitella CMOS-vastaanottimia valopulssin kulkuajan mittaukseen perustuvan lasertutkan integroituun vastaanotinpiiriin. Vastaanotinpiiri sisältää sekä vastaanotinkanavan että aika-digitaalimuuntimen yhdellä integroidulla sirulla. Tällöin systeemin integrointiastetta saadaan kasvatettua, mikä merkitsee esimerkiksi halvempaa hintaa ja pienempää tehon kulutusta.

Työssä on tutkittu vastaanotinkanavia, jotka käyttävät joko lineaariseen ilmaisuun tai etureunailmaisuun perustuvaa ajoitusilmaisutekniikkaa. Yleisesti vastaanotinkanava sisältää esivahvistimen, jälkivahvistimen ja ajoituskomparaattorin. Vastaanotetun signaalin tason voimakas vaihtelu saattaa aiheuttaa suuren systemaattisen virheen etureunailmaisuun perustuvassa ajoitusilmaisussa. Tässä työssä on esitetty etureunailmaisua käyttävä ajoitusilmaisin, jossa syntyvää ajoitusvirhettä voidaan korjata mittaamalla pulssin nousunopeutta aika-digitaalimuuntimella, joka on integroitu samalle sirulle. Aikatasossa tapahtuvan virheenkorjauksen etuna on mahdollisuus jatkaa virheenkorjausta amplituditasossa tapahtuvan signaalin leikkautumisen jälkeenkin, koska signaalin nousunopeus kasvaa leikkaantumisesta huolimatta.

Etureunailmaisua käyttävällä vastaanotinkanavalla, jossa ajoitusvirhettä korjattiin pulssin nousunopeutta mittaamalla, saavutettiin ±4,5 mm ajoitusvirhe 1:10000 dynaamisella alueella. Kertamittaustarkkuuden keskihajonta oli vähemmän kuin 25 mm, kun signaalikohinasuhde oli enemmän kuin 20. Vastaanotinkanavan käytettävyys osana lasertutkaa todettiin tekemällä tutkamittauksia kalibroidulla mittaradalla. Mittauksissa saavutettu lineaarisuus oli ±5 mm mittausalueen vaihdellessa 3 metristä 21 metriin ja signaalin dynamiikan ollessa enemmän kuin 1:2000.

Lisäksi työssä esitellään integroitu CMOS-pulssitin, joka pystyy tuottamaan ampeeri-luokan virtapulsseja laserdiodiin. CMOS-pulssittimella voitiin tuottaa 5 V käyttöjännitteellä ~1 A virtapulsseja optisen pulssin leveyden ja nousuajan ollessa ~2,5 ns ja ~1 ns.

*Asiasanat:* ajoitusilmaisu, CMOS-vastaanotinkanava, laserpulssitin, etäisyysmittaus

# Acknowledgements

This thesis is based on research work carried out at the Electronics Laboratory of the Department of Electrical Engineering and Infotech Oulu, University of Oulu, during the years 2002–2010.

At the beginning, I would like to thank my supervisor, Prof. Juha Kostamovaara, for excellent guidance and support during these long years and for educational conversations about the interesting world of the pulsed TOF laser rangefinders and the analogue electronics itself. I would like to thank my brother and co-worker Ilkka Nissinen for his help and support. I also thank my colleagues in the Electronics laboratory for the relaxing working atmosphere.

I wish to thank Prof. Torben Larsen and Prof. Sven Mattisson for reviewing this thesis and Malcolm Hicks for revising the English of the manuscript.

The work was supported financially by Infotech Oulu Graduate School, the Academy of Finland, the Finnish Funding Agency for Technology and Innovation (TEKES), Noptel oy, Polar Electro, National Semiconductor Finland and the foundations Tauno Tönningin säätiö, Tekniikan edistämissäätiö, Seppo Säynäjäkankaan tiedesäätiö, Nokia oyj:n Säätiö, Ulla Tuomisen Säätiö and Riitta ja Jorma J. Takasen säätiö, all of which are gratefully acknowledged.

I would like to thank my mother Pirkko and late father Raimo for their positive support during these years. My relatives and friends deserve also my gratitude for their support. Finally, I would like to express my warmest gratitude to my wife Teija and daughters Pinja and Inka for being the part of my life.

Oulu, September 2011 Jan Nissinen

# List of terms, symbols and abbreviations

The terms describing the performance of the measurement equipment are defined according to the IEEE Standard Dictionary of Electrical and Electronics Terms (IEEE 1996):

*Accuracy* is the degree to which a measured value agrees with the true value

*Jitter* is the short-term deviation of significant instants of a signal from their ideal positions in time

*Precision* is the quality of coherence or repeatability of measurement data, customarily expressed in terms of the standard deviation of an extended set of measurement results

*Resolution* is the least value of the measured quantity that can be distinguished

| | |
|---|---|
| ASIC | application-specific integrated circuit |
| AGC | automatic gain control |
| BiCMOS | bipolarCMOS, a semiconductor process containing bipolar and CMOS transistors |
| BW | bandwidth |
| CMOS | complementary metal oxide semiconductor |
| CFD | constant fraction discriminator |
| C-R | capacitor-resistor |
| DAC | digital-to-analogue converter |
| IC | integrated circuit |
| LCR | inductor-capacitor-resistor |
| MOSFET | metal oxide semiconductor field effect transistor |
| PWHM | pulse width at half maximum |
| RC | resistor-capacitor |
| RGC | regulated cascode |
| SNR | signal-to-noise ratio |
| TDC | time-to-digital converter |
| TOF | time-of-flight |

| | |
|---|---|
| c | speed of light |
| C | threshold two to threshold one ratio |
| $g_m$ | transconductance |
| $i_{peak}$ | peak value of the current pulse |

| | |
|---|---|
| $P_{rec}(R)$ | received power as a function of distance |
| $P_T$ | transmitted power |
| r | radius of the receiver lens |
| R | distance of the target |
| $t_{d1,d2}$ | delay between input and output signals at a specific threshold |
| $t_g$ | geometrical walk error |
| $t_p$ | timing point |
| $t_r$ | rise time |
| $t_{RC}$ | time constant of the receiver channel-dependent walk error |
| $t_{ro}$ | rise time of the optical pulse |
| $t_{r\_tot}$ | total rise time of the pulse |
| $v_n$ | noise voltage |
| $V_{in}$ | input voltage |
| $V_{max}$ | maximum voltage |
| $V_{out}$ | output voltage |
| $V_p$ | peak voltage of the pulse |
| $V_{thr}$ | threshold voltage |
| | |
| $\varepsilon$ | reflectivity of the target |
| $\Delta t$ | time difference between two thresholds |
| $\Delta t_{walk\text{-}res}$ | residual walk error |
| $\Delta t_{err}$ | walk error |
| $\Delta t_{err1}$ | walk error at the first threshold |
| $\Delta t_{err2}$ | walk error at the second threshold |
| $\sigma_t$ | timing jitter, standard deviation of measurements |
| $\sigma_v$ | noise power at the timing point |
| $\tau_R$ | transmission of the receiver optics |
| $\tau_T$ | transmission of the transmitter optics |

# List of original publications

This thesis is based on the following eight publications:

I Nissinen J, Palojärvi P & Kostamovaara J (2003) A CMOS Receiver for a Pulsed Time-of-Flight Laser Rangefinder. Proceedings of the IEEE European Solid-State Circuits Conference (ESSCIRC'2003). Estoril, Portugal, 16–18 Sep. 2003: 325–328.

II Nissinen J, Nissinen I, Palojärvi P, Mäntyniemi A & Kostamovaara J (2004) A CMOS Receiver Chip Consisting of a Receiver Channel and Time-to-Digital Converter for a Laser Radar. Proceedings of the 4th Topical Meeting on Optoelectronic Distance Measurement and Applications (ODIMAP'2004). Oulu, Finland, 16–18 June 2004: 164–169.

III Nissinen J & Kostamovaara J (2004) Wide Dynamic Range CMOS Receivers for a Pulsed Time-of-Flight Laser Range Finder. Proceedings of the IEEE Instrumentation and Measurement Technology Conference (IMTC'2004). Como, Italy, 18–20 May 2004, 2: 1224–1227.

IV Nissinen J & Kostamovaara J (2006) Fully Differential, Regulated Cascode Amplifier. Proceedings of the IEEE Mediterranean Electrotechnical Conference (MELECON'2006). Benalmadena, Spain, 16–19 May 2006: 51–54.

V Nissinen J & Kostamovaara J (2007) An Integrated Laser Radar Receiver Channel with Wide Dynamic Range. Proceedings of the IEEE International Conference on Electronics, Circuits and Systems (ICECS'2007). Marrakech, Morocco, 17–18 Dec. 2007: 10–13.

VI Nissinen J, Nissinen I & Kostamovaara J (2009) Integrated receiver including both receiver channel and TDC for a pulsed time-of-flight laser rangefinder with cm-level accuracy. IEEE Journal of Solid-State Circuits 44(5): 1486–1497.

VII Nissinen J & Kostamovaara J (2009) A 0.13 μm CMOS Laser Radar Receiver with Leading Edge Detection and Time Domain Error Compensation. Proceedings of the IEEE International Instrumentation and Measurement Technology Conference (I2MTC'2009). Singapore, 5–7 May 2009: 900–903.

VIII Nissinen J & Kostamovaara J (2009) A 1 A laser driver in 0.35 μm complementary metal oxide semiconductor technology for a pulsed time-of-flight laser rangefinder. Review of Scientific Instruments 80(10): 104703.

Papers I, III–V, VII and VIII were written by the author, who also carried out the practical work. Papers II and VI were written together with the second author, that the present author being responsible for the receiver channel part of the work. The author's work was supervised by Prof. Juha Kostamovaara, whose hints and ideas were helpful in ensuring its successful completion.

# Contents

# 1 Introduction

## 1.1 Aim of the work

The development of circuits for pulsed time-of-flight (TOF) laser rangefinding is one of the main areas of research at the Electronics laboratory of the University of Oulu. When work in this field started about 30 years ago (Ahola 1979), laser radars were constructed from discrete components and were large in size, as shown in Fig 1 a), a photograph of a laser radar developed for measuring lining wear in a converter (Määttä 1995). When application-specific integrated circuits (ASIC) gained in popularity and fabrication costs decreased, research became concentrated on reducing the size of laser radar devices by increasing their integration level (Palojärvi *et al.* 2002).

A pulsed TOF laser radar includes three main building blocks: an optical laser pulse generator, a receiver channel and a time interval measurement unit, or time-to-digital converter (TDC). Research work in the Electronics Laboratory has also been divided among these subareas. Developments of all the subareas have made it possible to construct more integrated components for laser radars, leading to substantial decreases in size and fabrication costs over the decades. The device shown in Fig. 1 b) is a laser radar of the proximity switch type which uses the TDC proposed by Räisänen-Ruotsalainen *et al.* (2000), and that in Fig. 1 c) is a laser radar receiver module using a integrated receiver channel (Palojärvi *et al.* 2005). A laser radar will typically include separate ASICs for the receiver channel and the time-to-digital converter (TDC), commercial discrete components, a microcontroller and a laser pulser, which is typically constructed using commercial discrete components.

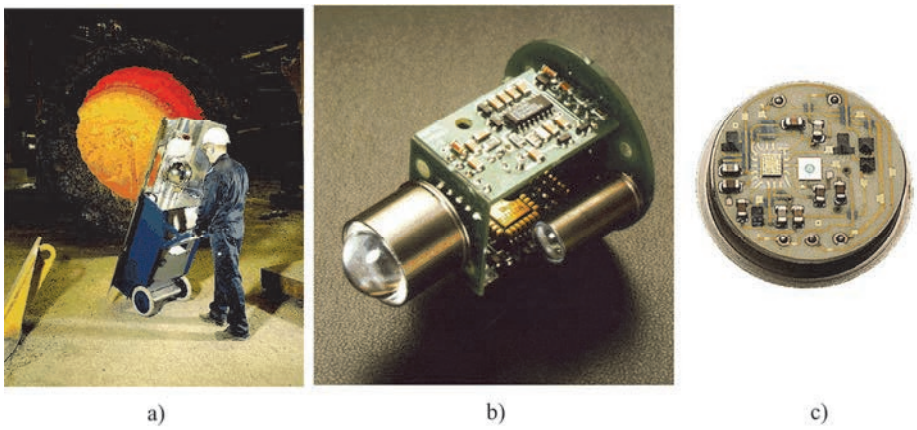


**Fig. 1. a), b) Laser radars and c) a laser radar module.**

The aim of this work was to increase the integration level further by fabricating a "laser radar chip" which would include both the receiver channel and the TDC on a single die fabricated in a standard CMOS technology. The leading technology in the digital design is CMOS because of the lower fabrication cost compared with BiCMOS technologies, for example, and the fact that TDCs have mainly been fabricated in standard CMOS technologies. On the other hand, high speed analogue designs have concentrated on BiCMOS because of the faster bipolar transistor and better achievable performance. The narrower line width of modern CMOS technologies has nevertheless made it possible to fabricate high performance analogue circuits as well, e.g. receiver channels, so that the integration level can be increased by including both the receiver channel and the TDC on the same CMOS chip, possibly resulting in reduced fabrication costs.

This thesis concentrates on the development of high performance CMOS receiver channels for laser radar receiver chips which also include the TDC. The main goal from the receiver channel point of view was to design one which could generate an accurate timing mark (<100 ps, i.e. 1.5 cm) for the TDC from an optical pulse with an amplitude varying over a 1:10 000… 100 000 dynamic range.

The laser pulse transmitter has typically been constructed using discrete components and typically requires a large supply voltage of hundreds of volts and a powerful driver, usually realized with a bipolar transistor working in the avalanche breakdown mode (Kilpelä & Kostamovaara 1997). The secondary goal of this work was thus to study the possibilities for constructing a semiconductor

laser diode driver which would produce an ampere-scale current pulse with a rise time of about one nanosecond in a standard CMOS technology with a low supply voltage.

It is believed that success in this research would pave the way for the development and fabrication of miniaturized laser radar micromodules for applications such as the positioning of tools and vehicles, the profiling and scanning of surfaces, anti-collision radars, proximity sensors and traffic perception devices, for example (Goldstein & Dalrymble 1967, Kostamovaara *et al.* 1992, Määttä *et al.* 1993, Kaisto *et al.* 1993, Kawashima *et al.* 1995, Araki & Yoshido 1996, Ng *et al.* 2004, Pananurak *et al.* 2008, Velupillai & Guvenc 2009).

## 1.2 Content and contribution of the work

The thesis is organized as follows. After the Introduction, Chapter 2 presents the pulsed TOF principle in more detail. It is divided into three subsections, each describing the operation of one of the main building blocks of a laser radar: the laser pulser, the receiver channel and the TDC.

Chapter 3 describes the timing discriminator problem. Variation in the amplitude of the optical pulse causes an amplitude-dependent timing error which detracts from the accuracy of the measurement. The origin of this timing error is explained and methods for avoiding it or compensating for it are explained together with their disadvantages and advantages. The requirements placed on the receiver channel are explained in Chapter 4.

The contribution of the original papers to this thesis is summarized in Chapters 5 and 6. Chapter 5 begins by presenting three alternative solutions for the CMOS receiver channel (Paper I, II and III). This is followed by a description of a fully differential regulated cascode transimpedance amplifier (Paper IV). After that a CMOS semiconductor laser diode driver for a pulsed TOF laser radar is presented in Paper VIII. The structure of the fourth receiver channel, fabricated in a 0.13 µm CMOS process, is explained in Chapter 6, and the feasibility of using the TDC to perform time domain timing error compensation is demonstrated in Papers V, VI and VII. Finally actual flight time measurements are presented to prove the suitability of the receiver channel fabricated in a 0.13 µm CMOS process for the application environment.

The proposed structures of the receiver channels and laser driver and the performance levels achieved with them are discussed and compared with previous work in Chapter 7. Finally, the work is summarized in Chapter 8.

The scientific contribution of the thesis is the development of CMOS receiver channels for an integrated pulsed TOF “laser radar chip” which includes both the receiver channel and the TDC on the same die. This kind of laser radar chip would be beneficial for industrial applications which require small size, low power consumption and low fabrication costs. Two leading edge timing discriminator-based receiver channels have been constructed with specific error compensation methods. The first uses conventional amplitude measurement to compensate for the timing error generated, and the other uses a new time domain timing error compensation method to achieve a wide dynamic range and small timing error. In addition, a low-voltage CMOS driver circuit for a semiconductor laser diode has been constructed. Finally, the achievable performance has been verified by inserting the “laser radar chip” into a full laser radar measurement setup and performing actual flight time measurements using a calibrated measurement track.

# 2 The pulsed time-of-flight laser rangefinder principle

A pulsed TOF laser rangefinder is based on measurement of the flight time of an optical pulse from a transmitter to the target and back to an optical detector, as shown in Fig. 2. Distance information can be calculated by means of the measured flight time and the known velocity of light. The device typically consists of a laser pulser with a semiconductor laser diode, two receiver channels, for the start and stop signals, and a unit to measure the time interval between the start and stop signals, as shown in Fig. 2.

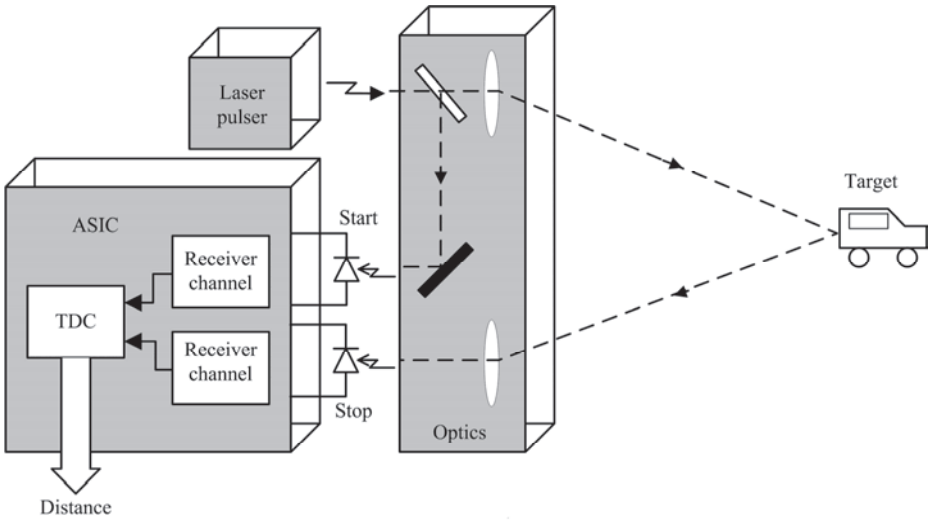


**Fig. 2. Principle of a pulsed TOF laser rangefinder.**

The semiconductor laser diode transmits a short optical pulse (2–6 ns) to the target and generates a timing event optically or electrically in the start channel, which amplifies the signal and eventually gives a logical timing mark for the TDC. In the same manner the optical echo is first received by an optical detector and then amplified by a stop channel to a suitable level for the TDC. The TDC converts the time difference between the start and stop signals to a digital word, which can then be converted to correspond to the distance from the target.

Pulsed TOF laser radars are widely used in many industrial, customer and military applications, for absolute distance measurements, the profiling and scanning of surfaces, velocity control, anti-collision radars, adaptive cruise control, traffic perception and automatic doors (Goldstein & Dalrymble 1967,

Kostamovaara *et al.* 1992, Määttä *et al.* 1993, Kaisto *et al.* 1993, Kawashima *et al.* 1995, Araki & Yoshido 1996, Ng *et al.* 2004, Pananurak *et al.* 2008, Velupillai & Guvenc 2009). The distance measurement range can vary greatly, from a couple of metres to several kilometres in military applications, for example, and the precision and accuracy requirements likewise depend on the application and can vary from a few millimetres to even metres. Pulsed TOF has advantages over other optical distance measurement techniques when fast measurements are needed, because it has the potential to give accurate results using only a single-shot measurement, the precision of which can be further improved by averaging several measurements.

Due to the high velocity of light, ~300 000 000 m/s, and the width of the optical pulse, 2–6 ns, some specific point in the transmitted pulse has to be detected in order to achieve sufficient accuracy, as a 67 ps timing error would correspond to 1 cm in distance. Moreover, the amplitude of the received echo can vary within a range of 1:100 000 depending on the distance to be measured, and large differences in reflection properties between clean, mirror-like metal plates and the muddy parts of a car surface in a traffic velocity control application, especially when aiming at centimetre-level accuracy, for example. These circumstances pose a challenge for the detection of the actual timing mark in the received echo.

A semiconductor laser diode is typically used as the transmitter in the pulsed TOF device, and when targeting a distance range of a few tens of metres with non-cooperative targets the peak power of the optical pulse should be at least in the range of several watts. On the other hand, to achieve an optical pulse width of a couple of nanoseconds at such a peak power level the driver electronics of the laser diode should be capable of generating short duration pulses at a high current level of several amperes. Conventional solutions have been based on the use of a power MOSFET or avalanche transistor as the switching device of the laser diode (Baker & Pocha 1990, Tsuchiya *et al.* 1981, Kilpelä & Kostamovaara 1997). Both structures require a high supply voltage of some hundreds of volts, however, in addition to which the gate capacitance of the power MOSFET can be of the order of several hundred picofarads, which requires a high current pre-driver in the switch device with a short rise time of a couple of nanoseconds. This can be a crucial disadvantage in some applications. A low voltage laser driver fabricated in a 0.35µm CMOS process is presented in this thesis to prove the ability of this technology to produce high current pulses through a semiconductor laser in order to achieve a peak power level which would be enough to measure distances of

several tens of metres. The laser diode driver is discussed in more detail in Chapter 5.4.

The purpose of the receiver channel is to amplify the varying amplitude current signal produced by the optical photodetector and to generate an accurate logic-level timing mark for the TDC. The receiver channel typically consists of a transimpedance preamplifier, a postamplifier and a timing discriminator (see Fig. 18 and 19). The simplest way of producing a timing mark for the TDC is to use a comparator with a constant threshold that changes stage when the amplitude of the leading edge of the pulse crosses the threshold. Unfortunately, this inevitably leads to an amplitude-dependent timing error, or walk error (Gedcke & Williams 1968, Arbel 1980: 194–205).

The linear range of the receiver channel is typically quite narrow, only about 1:100 ($i_{smax}$ to $i_{smin}$, corresponding to an SNR of 10). Automatic gain control circuits (AGC) can be used to increase the linear range and absorb the timing error caused by the amplitude variation. There are several methods for detecting the timing mark from a linear pulse signal, such as the well-known constant fraction discriminator (CFD) (Gedcke & McDonald 1967) or a C-R differentiator circuit (Simpson *et al.* 1995). Both these architectures generate an amplitude-independent timing mark as long as the amplitude of the signal is not disturbed in the channel, in other words as long as the linear range of the receiver is not exceeded. The dynamic range of the receiver channel which can be achieved in this way is less than 1:700 (Ruotsalainen *et al.* 2001). On the other hand, a leading edge timing discriminator benefits from the fact that the signal can be clipped in the amplitude domain and the large timing error caused by this can be compensated for by using some sort of information on the pulse strength, so that a large dynamic range can be achieved. The leading edge and linear timing discriminator schemes will be explained in more detail in Chapter 3.

The logic-level timing marks obtained from the receiver channels are passed to the TDC, which uses its time base to produce a digital word which represents the distance from the target. The details of the TDC lie beyond the scope of this thesis, in spite of its very important role in the time domain walk error compensation scheme proposed here (Chapter 3.3 and Papers VI and VII).

# 3 Timing discriminator

The timing discriminator is of vital importance from the timing detection accuracy point of view. One main problem is that the signal amplitude can vary greatly (even up to 1:100 000) depending on the reflectance properties of the target and the distance to be measured. It should also be kept in mind that the pulse width is a couple of nanoseconds, which corresponds in distance to approximately one metre. Thus some specific point in the pulse has to be detected in order to not to generate amplitude-dependent timing errors. There are basically two alternative solutions for generating the timing signal for the TDC: a leading edge timing discriminator and a linear timing discriminator. These two methods will be explained in this chapter together with their advantages and disadvantages and their sources of error.

## 3.1 Sources of error in timing detection

Errors in timing detection can be divided into two classes, systematic errors and statistical errors, the former usually being termed walk error and the latter timing jitter.

### *3.1.1 Jitter*

Jitter is caused by noise in the receiver channel and is always present regardless of the type of timing discriminator. The uncertainty in the timing moment caused by this noise is shown in Fig. 3 with two signal rise times and the same amount of noise. Using the triangle rule, the timing jitter $\sigma_t$, representing the standard deviation in the distribution of the measurement, can be calculated as (Bertollini 1968):

$$\sigma_t = \frac{\sigma_v}{\frac{d}{dt} v(t)\Big|_{t=t_p}}, \tag{1}$$

where $\sigma_v$ is the noise power at the timing point $t_p$ and v(t) is the input signal of the timing comparator. The jitter is largest when the signal is small and decreases as the signal is increased, because of the increased slew rate. If we take the SNR (peak signal current amplitude vs. rms noise) into account in (1), we can derive the formula

$$\sigma_t = \frac{\sigma_v}{\partial i_s / \partial t} \approx \frac{\sigma_v}{i_{peak} / t_{r\_tot}} \approx \frac{t_{r\_tot}}{SNR}, \quad (2)$$

where $i_{peak}$ is the signal amplitude and $t_{r\_tot}$ the rise time of the pulse in the channel. For reliable detection the SNR should be at least 10 (RCA 1974: 109–125, Ziemer & Tranter 1985, Määttä *et al.* 1993), so that with a receiver pulse rise time of 1.5 ns, for example, the maximum jitter will be approximately 150 ps. To reduce the jitter, the $t_{r\_tot}$ of the pulse should be minimized. On the other hand, the rise time of the pulse in the channel is

$$t_{r\_tot} = \sqrt{t_{ro}^2 + \frac{0.35^2}{BW^2}}, \quad (3)$$

where $t_{ro}$ is the rise time of the optical pulse and BW is the bandwidth of the channel. As the rms noise is proportional to √BW, there is an optimum jitter performance which can be aimed at by adjusting the rise time of the optical pulse and is achieved when BW = $0.35/t_{ro}$ (Ziemer & Tranter 1985, Ruotsalainen *et al.* 2001, Simpson & Paulus 1998). One advantage of the pulsed TOF method is that by averaging single measurements the jitter can be reduced by an amount inversely proportional to √N, where N is the number of asynchronous measurements averaged (Hewlett Packard inc.).

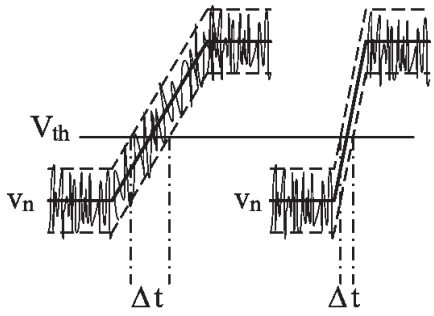


**Fig. 3. Jitter in timing discrimination.**

### *3.1.2 Walk error*

A systematic timing error, or walk error, always exists in timing discriminators of both types, but it is much larger in a leading edge timing discriminator, where a comparator, for example, is used to detect a signal when it exceeds a certain threshold, than it is in a linear timing discriminator. Thus, the varying amplitude of the reflected pulse causes an amplitude-dependent timing error in the timing moment, as shown in Fig. 4 (Gedcke & Williams 1968, Arbel 1980: 194–205).

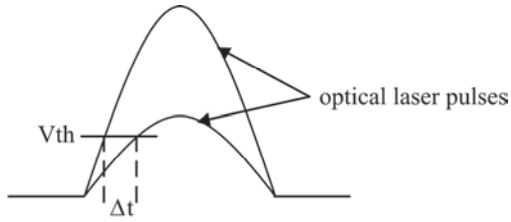


**Fig. 4. Walk error in a leading edge timing discriminator.**

The total walk error in leading edge detection can be divided into two parts: the geometrical walk error and the error caused by the finite bandwidth of the receiver channel and timing comparator. The total walk error can be approximated by comparing the delays in the amplitude responses of the minimum and maximum signals. The amplitude responses of the receiver channel with small and large signals are shown in Fig. 5, where the geometrical walk error, $t_g$, always exists in the timing discriminator even given an ideal receiver. According to Fig. 5, $t_g$ can be represented as

$$t_g = \frac{V_{th}}{V_p} \cdot t_r, \tag{4}$$

where $t_r$ is the rise time of the pulse and $V_{th}$ and $V_p$ are the threshold voltage and the peak voltage of the received pulse, respectively. The geometrical walk error is due to the finite rise time of the pulse and can be minimized by reducing the rise time of the optical pulse. This has only a limited effect, however, because in the last resort even in a step pulse it is the bandwidth of the receiver channel that sets the rise time of the detected pulse, to a finite value which is inversely proportional to the bandwidth.

The walk error that is dependent on the time constant of the receiver channel, $t_{RC}$ in Fig. 5, can be evaluated as being proportional to the difference between the

time delays in the receiver channel with small and large input pulses. For a small pulse the $t_{RC}$ is approximately that of the RC of the receiver channel, and with the maximum signal this delay is negligible. Thus the total error is equal to the RC, so that the total walk error can be estimated to be $t_g + t_{RC}$. The rise time of the optical pulse is typically in the nanosecond range, and with a receiver channel of bandwidth 250 MHz, for example, the total walk error can be as large as 1–2 ns, which correspond in distance to 15–30 cm (Palojärvi 2003, Palojärvi *et al.* 2005, van de Plassche 1994: 189–199, van de Plassche & Baltus 1988).

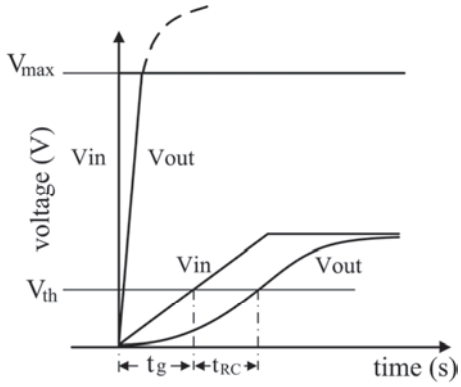


**Fig. 5. Walk error in a leading edge timing discriminator (VI, published by permission of IEEE).**

## 3.2 Point of departure for the present work

As explained above, the walk error in leading edge timing discrimination can be in the nanosecond range. This large error is not acceptable for accurate rangefinding, but there are a couple of solutions for avoiding the walk error or compensating for it in order to achieve better accuracy. These will be discussed in more detail below.

Several methods have been proposed for avoiding walk error, one of which is based on the use of automatic gain control to absorb the variation in the amplitude of the signal in order to achieve an accurate timing mark. Without the any pulse shaping scheme, however, the dynamic range would be limited to 1:15 (Ruotsalainen *et al.* 1999a). One way to extend the dynamic range would be to produce a bipolar pulse electrically from the unipolar optical pulse so that it would then have an amplitude-independent zero crossing point, as shown in Fig. 6

(Simpson *et al.* 1997). The zero crossing point of varying-amplitude bipolar pulses will remain stable as long as the pulses are processed linearly.

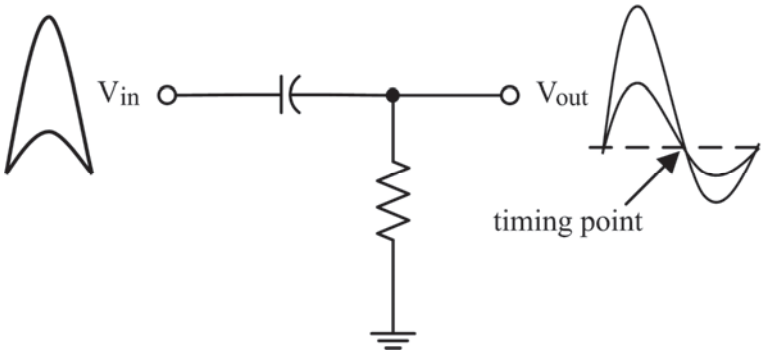


**Fig. 6. A C-R filter for producing a bipolar pulse from a unipolar optical pulse.**

One method for producing a timing arrangement of this kind in an integrated receiver channel is to use a simple C-R high-pass filter located at the input of the comparator. The filter and the shapes of the pulses before and after it are shown in Fig. 6. With automatic gain control a dynamic range of 1:700 has been achieved with a ±4 mm timing error (Ruotsalainen *et al.* 2001, Palojärvi *et al.* 2002).

To achieve a greater dynamic range, unipolar-to-bipolar conversion can be moved from the output of the amplifier channel to the input of the receiver channel. Pehkonen & Kostamovaara (2003) and Pehkonen *et al.* (2006), for example, made this conversion by means of an LCR resonator circuit at the input of the receiver channel, in which case a dynamic range of approximately 1:1300 was achieved with a timing error of 74 ps, i.e. ±5.5 mm. A current buffer has also been used as the input stage, and the high-pass filter has been located after that to achieve a greater dynamic range (Kurtti & Kostamovaara 2005, Kurtti & Kostamovaara 2009a). The former receiver channel achieved a timing accuracy of 110 ps (± 8 mm) within a dynamic range of 1:1600 and the latter 110 ps (± 8 mm) within a dynamic range of 1:3000. Moreover, these techniques used no gain control to achieve the above performances. All these receiver channels based on the linear timing discriminator scheme have been fabricated in BiCMOS technologies.

If the aim is to achieve larger dynamic range than 1:3000 a leading edge timing discriminator is the most practical solution. The problem, however, is that

a large timing error occurs, as explained in the previous chapter. Several methods have been developed to compensate for this timing error by measuring certain properties of the received pulse, such as its amplitude or width. One possible structure for compensating for the walk error is to use information gained from measuring the amplitude of the received pulse with a peak detector, but this calls for accurate amplitude measurement circuitry (Ruotsalainen 1999b) and works only when the pulse amplitude is within the linear range of the receiver channel, so that its value can be measured. This means that the dynamic range is limited. The above method has been used by Peltola *et al.* (2000) and Palojärvi *et al.* (2005) to achieve a walk error of ±35 mm within a dynamic range of 1:4000. Amplitude measurement was also used in Paper I of this thesis, but the amplitude was measured not only after the postamplifier but also after the preamplifier, so that the linear range of the amplitude measurement could be increased. This work is presented in more detail in Chapter 5.1. Other parameters of the pulse can also be measured to compensate for walk error (Lim & Park 2003). Kurtti & Kostamovaara (2009b) and Kurtti & Kostamovaara (2011) measured the width of the pulse and used this to correct the timing error within a very wide dynamic range of 1:100 000 with a timing error of only ±3 mm.

The advantages of leading edge timing discriminators are their large dynamic range, even exceeding the linear dynamic range of the receiver, as will become obvious later in this thesis, and their simple structure. A linear timing discriminator scheme is very accurate because it generates a minimum amount of geometrical walk error, but it suffers from a lack of dynamic range. Thus there is a trade-off between dynamic range and the accuracy needed, and the best solution depends in general on the application involved.

## 3.3 A leading edge timing discriminator with time domain error compensation

As described in the previous chapter, the leading edge timing discriminator has the advantage of a wide dynamic range, but its timing error is too large without any compensation. A conventional compensation method such as an amplitude measurement can be used to produce an accurate timing mark, but only in a limited range of less than 1:3000 (Palojärvi *et al.* 2005). In addition, the evenly reducing linear range in modern narrow line width IC technologies places strict accuracy requirements on the amplitude measurement circuitry. In some applications, however, the signal amplitude can vary over a range of 1:10 000 or

even more. This is true of collision avoidance applications, for example. Thus the receiver channel has to be able to produce a timing mark even when the signal level saturates the receiver channel. In view of these facts, a time domain error compensation principle was designed here to achieve accurate timing detection with a large dynamic range and without the use of any gain control scheme. This compensation method also benefits from the fact that the timing resolution of modern IC processes is improving even though the supply voltage, and thus the linear range of the receiver, is being reduced.

### *3.3.1 Accuracy of time domain error compensation*

The basic idea of this compensation approach is to measure not only the timing moment of the crossover point of the timing pulse at a certain threshold but also the slew rate of the leading edge of the timing pulse by means of two comparators with different thresholds, as shown in Fig. 7 a). The known relationship of the slew rate of the pulse to the walk error can now be used to compensate for the resulting timing error. As the amplitude of the signal increases, the time difference between the two thresholds decreases, as does the walk error, as can be seen in Fig. 7 b). Thus we have a monotonic dependence between these two parameters. The main benefit is that the compensation can be continued even though the linear range of the receiver has been exceeded, because the slew rate of the front end of the pulse continues to increase even then. According to Fig. 7 b), the time difference between the two thresholds for an idealized linear signal ramp can be written as

$$\Delta t = \frac{(C-1)\cdot t_r \cdot V_{thr}}{V_p}, \tag{5}$$

where C is the ratio between the upper and lower thresholds, $t_r$ the rise time of the receiver output pulse and $V_p/V_{thr}$ the ratio between the signal amplitude and the lower threshold setting. The walk error at a specific amplitude can be defined as

$$\Delta t_{err} = \frac{t_r \cdot V_{thr}}{V_p}. \tag{6}$$

Combining these two equations, we can set a limit for the minimum residual walk error with a specific time interval measurement resolution Δt, resulting in $\Delta t_{walk\_res}=\Delta t/(C-1)$. Thus the residual walk error is directly proportional to the

resolution of the time interval measurement. With a 10 ps resolution and C = 2, for example, the residual walk error would be 10 ps.

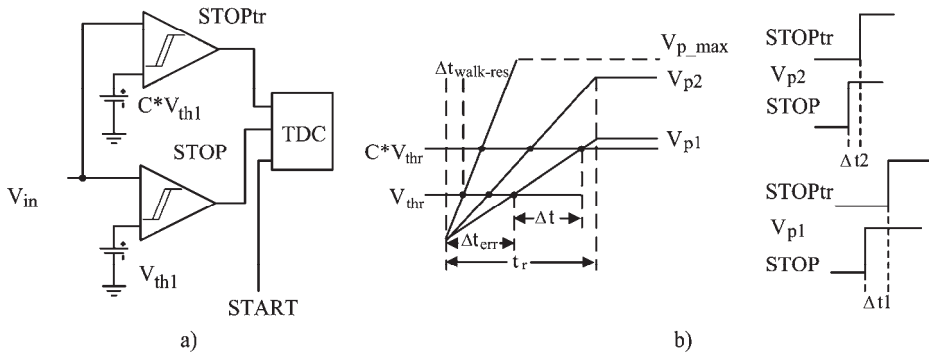


**Fig. 7. a) The basic idea of time domain error compensation, and b) ideal waveforms.**

A more sophisticated model for analysing the accuracy of the compensation that also includes the effect of the receiver channel delay is shown in Fig. 8. This model also takes into account the delay variation caused by the time constant RC of the receiver channel. Using the notations of Fig. 8, we obtain for Δt and the walk errors

$$\Delta t_{err1} = \frac{V_{thr}}{V_p} \cdot t_r + t_{d1}, \tag{7}$$

$$\Delta t_{err2} = C \cdot \frac{V_{thr}}{V_p} \cdot t_r + t_{d2}, \tag{8}$$

$$\Delta t = \Delta t_{err2} - \Delta t_{err1} = \frac{V_{thr}}{V_p} \cdot t_r \cdot (C-1) + t_{d2} - t_{d1}, \tag{9}$$

where $t_{d1,\ d2}$ are delays between the input and output at a specific threshold. According to van de Plassche (1988), $t_{d1,\ d2}$ can be written as

$$t_{d1} = RC \cdot (1 - e^{-\left(\frac{V_{thr}}{V_p} \cdot t_r + t_{d1}\right)/RC}), \tag{10}$$

$$t_{d2} = RC \cdot (1 - e^{-\left(C \cdot \frac{V_{thr}}{V_p} \cdot t_r + t_{d1}\right)/RC}), \tag{11}$$

where RC is the time constant of the receiver channel. The delays $t_{d1,\ d2}$ can be solved using second-degree series development of the exponent function, and are

$$t_{d1} \approx -\frac{V_{thr}}{V_P} \cdot t_r + \sqrt{2 \cdot RC \cdot \frac{V_{thr}}{V_P} \cdot t_r}, \tag{12}$$

$$t_{d2} \approx -C \cdot \frac{V_{thr}}{V_P} \cdot t_r + \sqrt{2 \cdot RC \cdot C \cdot \frac{V_{thr}}{V_P} \cdot t_r}\ . \tag{13}$$

To analyze the effect of the measurement resolution Δt on the final accuracy of the compensated walk error in the result $\Delta t_{err1}$ has to be solved as function of Δt. By inserting the results of (12) and (13) into (9) $V_{thr}/V_p$ can be solved as a function of Δt. Then, by inserting the answer and (12) into (7), the walk error as a function of Δt can be presented as

$$\Delta t_{err1} = \frac{\Delta t}{\sqrt{C} - 1}. \tag{14}$$

Thus, with a resolution of 10 ps and C values of two and three, for example, the residual walk errors will be 24 ps and 14 ps, respectively.

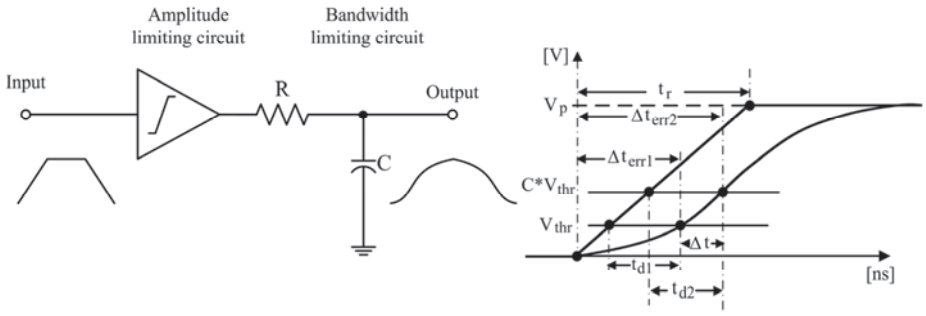


**Fig. 8. Model for analysing error caused by time domain walk error compensation.**

To achieve a more accurate understanding of the effects of the comparator threshold settings and the resolution of time interval measurement on the achievable accuracy, Matlab simulations were carried out to take into account the effect of the finite bandwidth of the receiver channel and saturation of the channel. The receiver channel used in the simulation was modelled by a one pole and an amplitude-limiting circuit which models the receiver channel entering the saturation region. The bandwidth of the receiver channel was approximately 250

MHz and the rise time of the ramp pulse was 2 ns (100%). The thresholds of the comparators were set to 0.45 and 0.9 when the minimum detectable signal was one (0.45 corresponds SNR=10 i.e. rms-noise is 0.045). The walk error (change in the timing point at the 0.45 threshold, grey line) and the timing difference between the two threshold settings, Δt (black line), are shown as functions of the input amplitude in Fig. 9. As can be seen in the zoomed plot in Fig. 9, Δt still decreases in amplitude level from 1000 to 10000 and is 10 ps at an amplitude of 2000. The residual walk error at that amplitude is approximately 25 ps, as expected from (14) if the resolution of the time interval measurement unit is 10 ps.

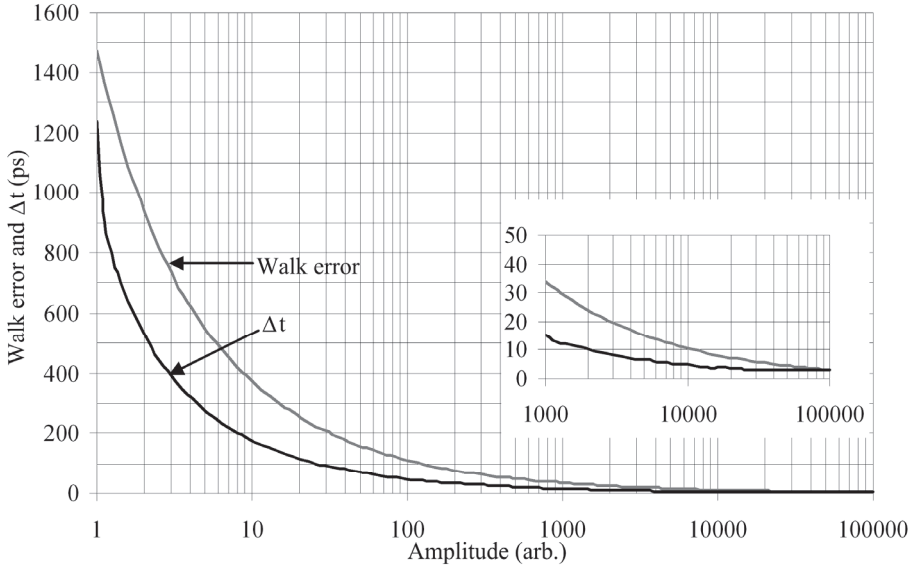


**Fig. 9. Walk error (grey) and Δt (black) as functions of pulse amplitude (C = 2).**

Another simulation was carried out using threshold settings of 0.45 and 1.35 and a minimum signal of 1.5 to ascertain how a change in threshold settings would affect the residual walk error. As seen in Fig. 10, the residual walk error is now 14 ps (@7000) and has been reduced by a factor of 1.8, as predicted by equation $\Delta t_{walk\text{-}res}=\Delta t/(\sqrt{C}-1)$. On the other hand, the minimum detectable signal was increased by a factor of 1.5 because of the larger threshold of the second comparator.

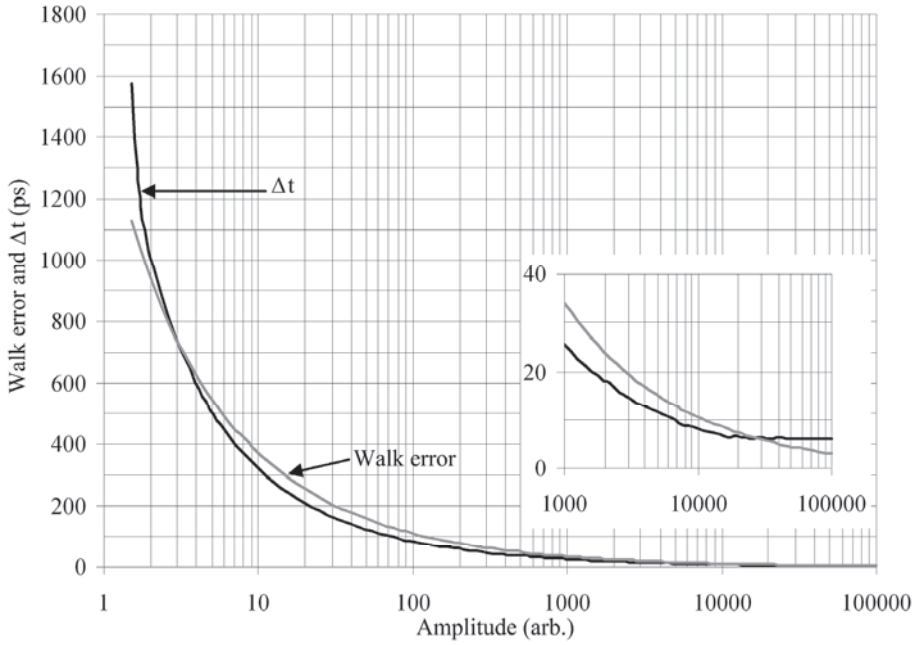


**Fig. 10. Walk error (grey) and ∆t (black) as functions of pulse amplitude (C = 3).**

### *3.3.2 Single-shot precision of time domain error compensation*

The same simulation setup was also used to analyse the jitter properties of the leading edge timing discriminator with the time domain error compensation scheme. The receiver channel was modelled by two poles instead of the one pole used in the former simulation in order to obtain more realistic results. Noise in the receiver channel and the uncertainty of the TDC were included in the model to ascertain their impact on the precision of the compensation method. The rms noise value was selected to give an SNR of 10 at the lower threshold of 0.45. In single-threshold leading edge detection the jitter is proportional to the ratio of the receiver noise to the slew rate of the timing signal at the timing point, as shown in (1). Using two comparators with different thresholds to produce timing marks for the TDC, the jitter of the individual comparator is as large as that shown in (1). Thus the jitter in the measured slew rate is affected by the noise at the threshold levels of both comparators. The jitter in the slew rate measurement affects the total precision of the compensated result via the slope of the compensation curve,

as is shown in Fig. 11. Now the total single-shot precision of the proposed compensation principle depends on the jitter produced by the first comparator, as in conventional leading edge detection, and on the jitter of the Δt measurement, via the slope of the compensation curve. The compensation curve used in the simulation was that defined in the previous simulation, which shows the walk error as a function of the Δt measured between two thresholds. Compensation curves with C values of two and three are shown in Fig. 11. Two simulations were carried out, one with each value of C, to assess the effects of the threshold settings on jitter properties.

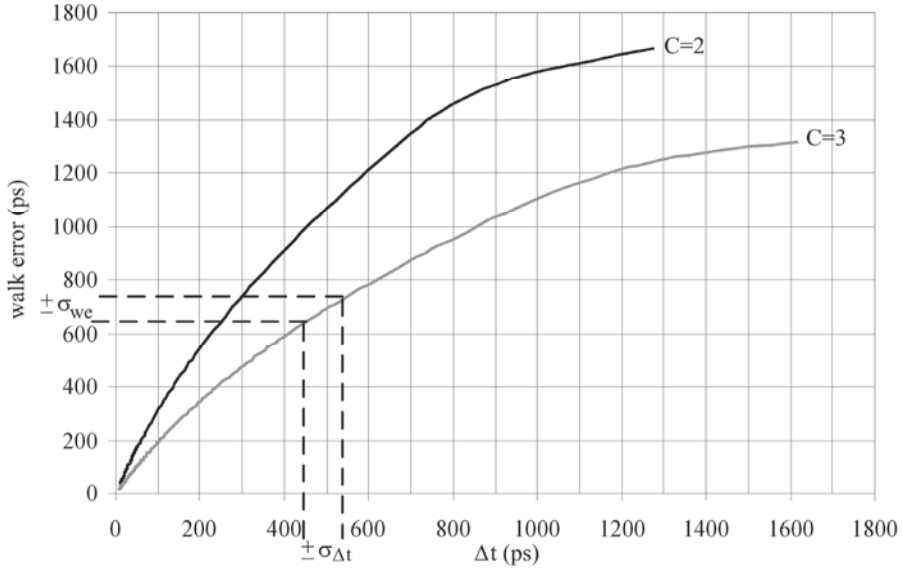


**Fig. 11. Compensation curves with C values of two and three.**

The simulated single-shot precision as a function of signal amplitude is shown in Fig. 12 with and without compensation (500 simulations averaged at each amplitude) and with two threshold settings. As seen in Fig. 12, the precision of the conventional structure (dotted line) saturates to the value of the uncertainty of the TDC, which was about 15 ps in the simulation, while the precision of the proposed compensation method saturates to values of about 60 ps (C = 2) and 40 ps (C = 3) depending on threshold settings, because of the different slopes of the compensation curves. The single-shot precision can be improved by using the

larger ratio of three between the threshold settings, which can be intuitively explained by the lower slope of the compensation curve (see Fig. 11). The peaks of the curves in Fig. 12 with low-amplitude signals are due to the change in the gradients of the compensation curves when $\Delta t$ is approximately 850 ps with a C of two and 1200 ps with a C of three. Although precision is degraded by using the proposed structure, the systematic, amplitude-dependent walk error can be reduced to tens of picoseconds as compared with the nanosecond range achievable with the conventional leading edge timing discriminator without any compensation, as is shown in Fig. 13.

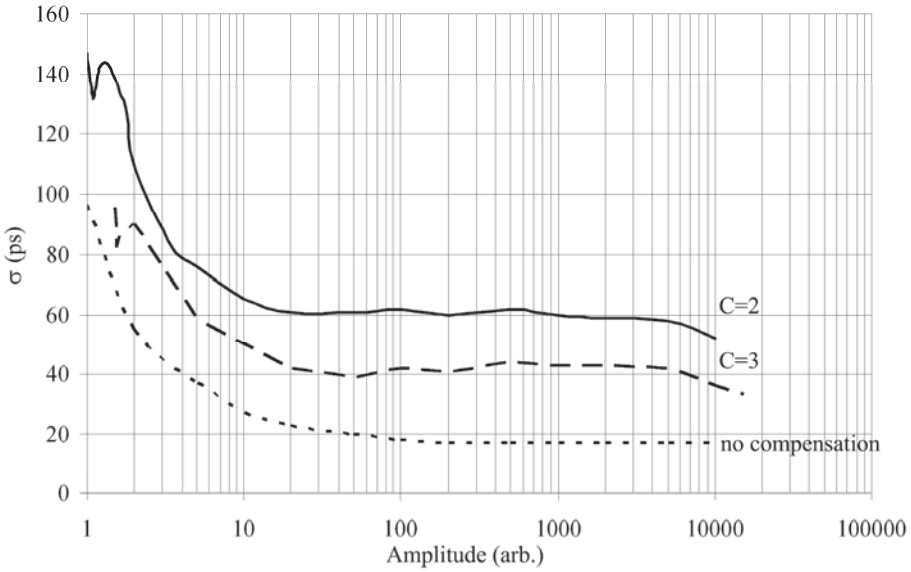


**Fig. 12. Single-shot precision of leading edge detection with the time domain error compensation scheme.**

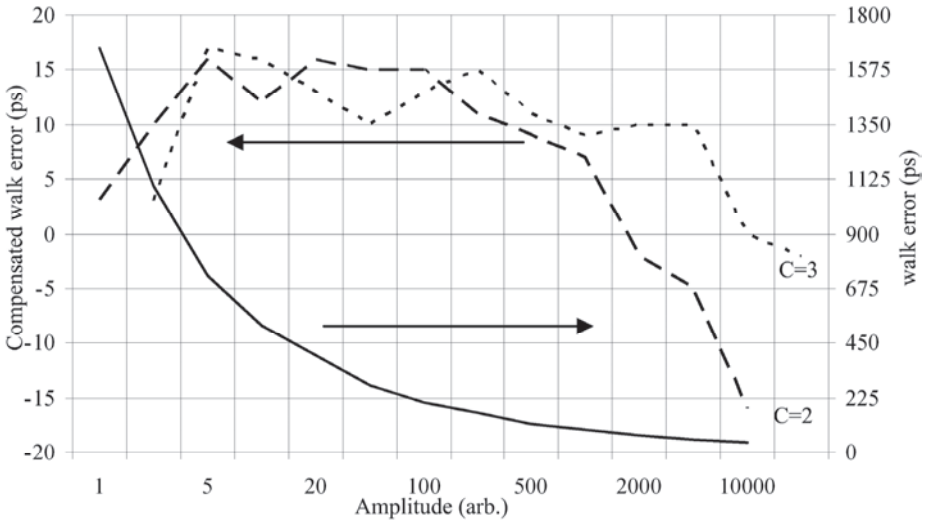


**Fig. 13. Walk error without (solid line) and with time domain compensation, given C values of two (dashed line) and three (dotted line).**

In the above jitter simulations the slew rate of the channel was infinite, so that compensation could be continued until the minimum measurable Δt was limited to approximately 10 ps by the resolution of the TDC. To analyse the effect of slew rate limitation, a rate-limiter block was included in the Matlab simulation model and the amplitude was swept from one to 10 000 with two values of C, two and three. The minimum Δt between the thresholds 0.45/0.9 and 0.45/1.35 was limited to 30 ps and 60 ps, respectively. The single-shot precision as a function of amplitude is shown in Fig. 14. Taking the slew rate limitation into account, the single-shot precision starts to deteriorate due to saturation of the minimum measurable Δt, which causes a larger error in the compensation at higher signal amplitudes. This can also be explained by the deeper slope of the compensation curve at the smaller measured values of Δt, as is shown in Fig. 15 and is also seen in the experimental results quoted in section 6.2.1.

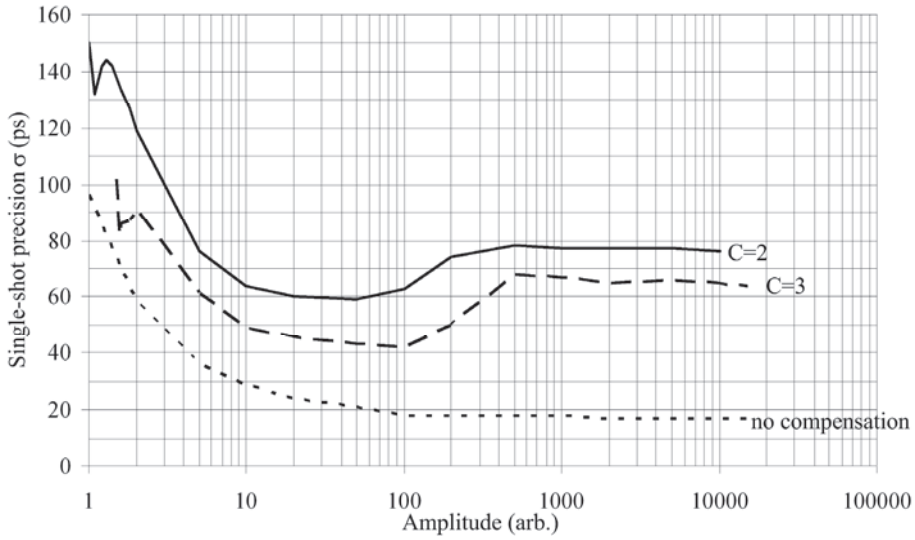


**Fig. 14. Single-shot precision with the slew rate limitation model used in the simulation.**

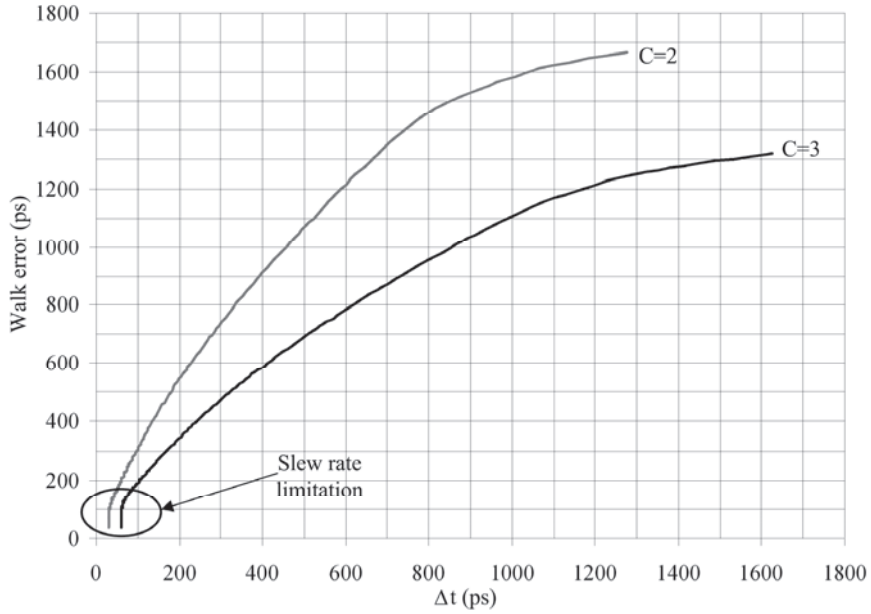


**Fig. 15. Compensation curves with slew rate limitation, using C values of two (grey) and three (black).**

# 4 Requirements for the receiver channel

The performance achievable with pulsed time-of-flight laser rangefinder techniques is affected by the performance of the laser pulser, receiver channel, optics and TDC. The typical requirements for the receiver channel will be examined here with regard to the desired performance.

## 4.1 Bandwidth

The optical pulse widths (PWHM) which can be generated with a semiconductor laser diode with a sufficient peak power level to measure distances up to twenty metres or so are typically 2–6 ns, with a rise time of 1–3 ns (Kilpelä & Kostamovaara 1997). Thus, in order to achieve the best possible jitter properties in the receiver channel with the rise time of the optical pulse used here, the bandwidth should, according to Chapter 3.1, be $0.35/t_{ro}$, which is approximately 250 MHz with a rise time of 1.4 ns, for example.

When aiming at cm-level precision the jitter in timing discrimination should be less than 70 ps. If the rise time of the pulse at the input to the timing comparator is limited by the bandwidth of the receiver channel, the single shot precision given by (1) can be approximated in leading edge detection by (Kostamovaara *et al.* 1992, Ruotsalainen 1999b)

$$\sigma_R = \frac{0.35 \cdot c}{2 \cdot BW \cdot SNR}, \tag{15}$$

where c is the speed of light, BW is the bandwidth and SNR is the peak signal voltage to rms noise voltage ratio. As mentioned in the previous chapter, an SNR of at least 10 should be used to prevent false triggering. According to (15), cm-level precision can then be achieved with a bandwidth of at least 500 MHz. When using the time domain error compensation scheme the minimum signal should correspond to an SNR of 20 (C = 2), in which case the minimum bandwidth should be at least 250 MHz to achieve cm-level single shot precision.

## 4.2 Noise

The measurement range which can be achieved is limited by the noise in the receiver channel, because the optical power received decreases in a manner that is inversely proportional to the squared distance R, according to the radar equation

$$P_{rec}(R) = \frac{P_T \cdot \tau_T \cdot \varepsilon}{\pi} \cdot \frac{\pi \cdot r^2}{R^2} \cdot \tau_R , \qquad (16)$$

where $P_\tau$ is the output power of the laser diode, $\tau_T$, $\tau_R$ are the transmission of the transmitter and receiver optics, respectively, ε is the reflectivity of the target and r is the radius of the receiver lens. The received peak power together with the responsivity of the optical detector (an avalanche photodiode, typically R~30 A/W) defines the input current of the receiver channel. For a typical receiver bandwidth of 200…300 MHz, the equivalent input noise current is around 50…100 $nA_{rms}$, which means that the minimum signal current is about 1 μA at the required minimum SNR of 10.

In a good design the noise performance of the receiver channel is mainly limited by the preamplifier, which is usually a transimpedance amplifier, because the signal from the photodetector is in current form. The transimpedance amplifier will typically include a voltage amplifier and a feedback resistor, as shown in Fig. 16.

The dominant noise sources of this configuration are the thermal noise of the feedback resistor and the input-referred voltage noise of the voltage amplifier, also shown in Fig. 16. Ignoring the 1/f noise, the input-referred current noise power spectral density can be written as

$$i_{nineq}^2(\omega) = \frac{4kT}{R_f} + \frac{8}{3} \cdot \frac{kT}{g_m \cdot R_f^2} \cdot \left[1 + \left(\omega \cdot R_f \cdot C_{inT}\right)^2\right] . \qquad (17)$$

The first term in (17), representing the thermal noise of the feedback resistor, is dominant at low frequencies, while the second term, which is attributable to the voltage noise of the input transistor, starts to increase at higher frequencies because of the zero in the transfer function caused by the input capacitance $C_{inT}$. To minimize both terms, $R_f$ and $g_m$ should be maximized and the input capacitance should be minimized. Increasing $g_m$ will also affect the input capacitance, however, and thus there is an optimum size for the input transistor which gives the minimum noise (Abidi 1987, Ingels & Steyaert 1999, Säckinger 2005). As the bandwidth of the preamplifier is inversely proportional to $R_f/A$, maximizing $R_f$ will degrade the bandwidth, although this can be compensated for by increasing the gain A of the voltage amplifier. As a result, improving the gain A also improves the noise performance. The total amount of rms noise at the output matters in laser radar applications, because the signal is corrupted by it.

Thus it is also important to limit the bandwidth of the voltage amplifier within the bounds of stability to reduce noise at higher frequencies (Säckinger 2005) or to limit the bandwidth properly at the postamplifier.

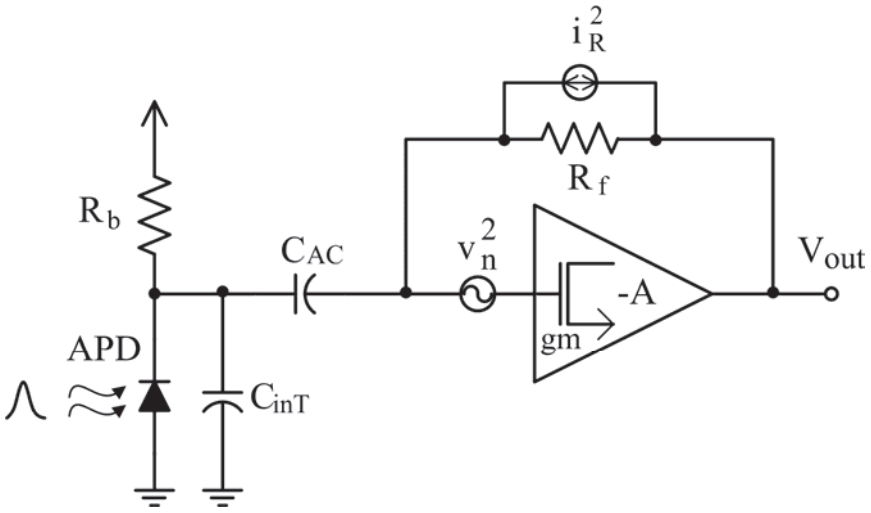


**Fig. 16. The transimpedance preamplifier with its dominant noise sources.**

# 5 Reviews of the papers

## 5.1 A receiver channel with a leading edge timing discriminator and amplitude domain error correction (Papers I and II)

Papers I and II present a receiver channel fabricated in a 0.35 μm CMOS technology. The chip also includes an on-chip TDC (Nissinen I *et al.* 2003). The receiver is based on a leading edge timing discriminator and the resulting walk error is compensated for by means of peak detectors and amplitude measurement. A photograph of the ASIC is shown in Fig. 17.

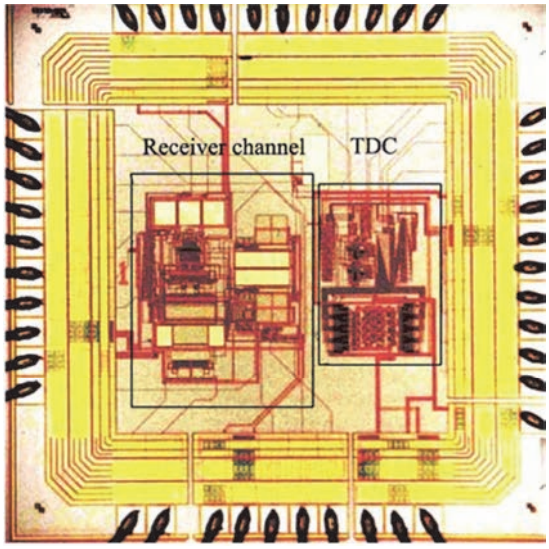


**Fig. 17. Photograph of the receiver designed in a 0.35 μm CMOS process (I, published by permission of IEEE).**

The receiver channel consists of a transimpedance preamplifier, a postamplifier and a leading edge timing discriminator. In addition, two peak detectors are used to measure the amplitude of the signal, and that information is used to compensate for the walk error. The first peak detector is located after the preamplifier and the second one after the postamplifier. The dynamic range of the compensation can be increased by using the information on the amplitude of the peak detector after

the preamplifier when the peak detector after the postamplifier starts to saturate in the amplitude domain.

The measurements obtained for the receiver channel, described in Papers I and II, proved that both the receiver channel and the time-to-digital converter can be implemented on the same chip without significant deterioration in performance, showing that the development of a single chip realization was reasonable and its advantages, such as a smaller size and lower power consumption, could be exploited in future work.

## 5.2 Receiver channels with a linear timing discriminator (Paper III)

Paper III describes two receiver channels based on a linear timing discriminator scheme simulated in a 0.18 μm CMOS technology with a 1.8 V power supply. In the first channel unipolar-to-bipolar conversion was performed by a two-stage C-R network at the input of the receiver. After that the bipolar signal was amplified by cascaded voltage amplifiers to a suitable level for the timing discriminator. The second channel used a regulated cascode front end as a current buffer followed by a C-R high-pass filter which converted the unipolar pulse to a bipolar one. The back end of the channel was similar to that in the first design. Simulations showed that in this CMOS technology the dynamic range of the linear timing discriminator scheme was limited to 1:1000 with a timing error of approximately 120 ps, equivalent to a distance of ±10 mm. In an application such as a collision avoidance system such a dynamic range would be inadequate, which directed the research towards leading edge timing discriminators.

## 5.3 A fully differential, regulated cascode amplifier (Paper IV)

In Paper IV a fully differential, regulated cascode (RGC) amplifier was proposed and simulated in a 0.18 μm CMOS technology. RGC stages have been recommended for use in optical telecommunications where high bandwidth is needed to achieve a high bit rate (Park & Toumazou 1998, Park & Yoo 2004). The proposed structure achieved lower noise and input impedance by means of the differential input signal from the photodetector, contrary to the conventional structure, where a single-ended photodetector is usually used. This structure achieved an especially good reduction in the effect of the voltage noise of the feedback transistor, which is the dominant noise source.

## 5.4 A laser pulser realized in a 0.35 µm CMOS technology (Paper VIII)

As explained in the introduction, short optical pulses have to be used to achieve good timing resolution and small walk error. To generate optical pulses with a rise time of less than a few nanoseconds requires a very fast switching device to drive the semiconductor laser. Conventional structures for generating short semiconductor laser pulses are typically based on an avalanche transistor, a power MOSFET or a step recovery diode (Kilpelä & Kostamovaara 1997, Baker & Bocha 1990, Howard & Daneshvar 1989). The drawbacks with these devices are that they need a high voltage source (~200 V) and high current driver to switch the device on fast enough to generate short pulses.

The integrated CMOS laser diode driver circuit fabricated in a 0.35 µm CMOS technology proposed in Paper VIII includes four parallel NMOS transistors and a gate driver, which is a simple scaled buffer chain for achieving fast switching. A parallel structure has been used to minimize the inductances of bonding wires (Thompson & Schlecht 1997, Wens *et al.* 2009).

Measurements showed that a peak current pulse with an amplitude of ~1 A, optical pulse width of ~2.5 ns and rise time of ~1 ns could be achieved with the proposed structure and a 5 V power supply. Using the Thorlabs L904P030 laser diode an optical peak power of approximately 450 mW was achieved with a rise time of 1 ns, and this could be further increased by 50% with a small pre-bias current of 1.5 mA through the laser diode. To achieve sufficient optical power to measure distances of twenty metres or so in the case of non-cooperative targets, special high-voltage CMOS processes have to be used to provide a larger supply voltage to the laser diode. Detailed measurements performed on the laser pulser are presented in Paper VIII.

# 6 Implementation of a receiver for a pulsed TOF laser rangefinder micromodule (Papers V, VI and VII)

The knowledge acquired with these earlier designs oriented the research towards the use of leading edge detection in timing discrimination to achieve a sufficient dynamic range. In addition, these results demonstrated that the receiver channel and time-to-digital converter can be implemented on the same CMOS chip while still obtaining the necessary performance.

The receiver channel presented in this chapter and in papers V, VI and VII was fabricated in a 0.13 μm CMOS technology and is based on leading edge timing discrimination with time domain walk error compensation. The chip also includes a two-channel TDC (Nissinen I & Kostamovaara 2009). Because of the lack of linear range in the amplitude domain which is especially emphasized in modern IC technologies, walk error compensation in this domain has a limited achievable dynamic range, so that if cm-level accuracy were aimed at, for example, a dynamic range of about 1:500 could be achievable. Time domain walk error compensation benefits from the fact that the TDC is already available in the device and needs only slight modification, one extra channel, to perform the compensation, but an important further advantage is its wide dynamic range, because compensation can be continued even though the signal is saturated in the amplitude domain. In addition, this compensation scheme also works for single-shot measurements. A block diagram of the whole receiver chip including the I/O-connections is shown in Fig. 18.

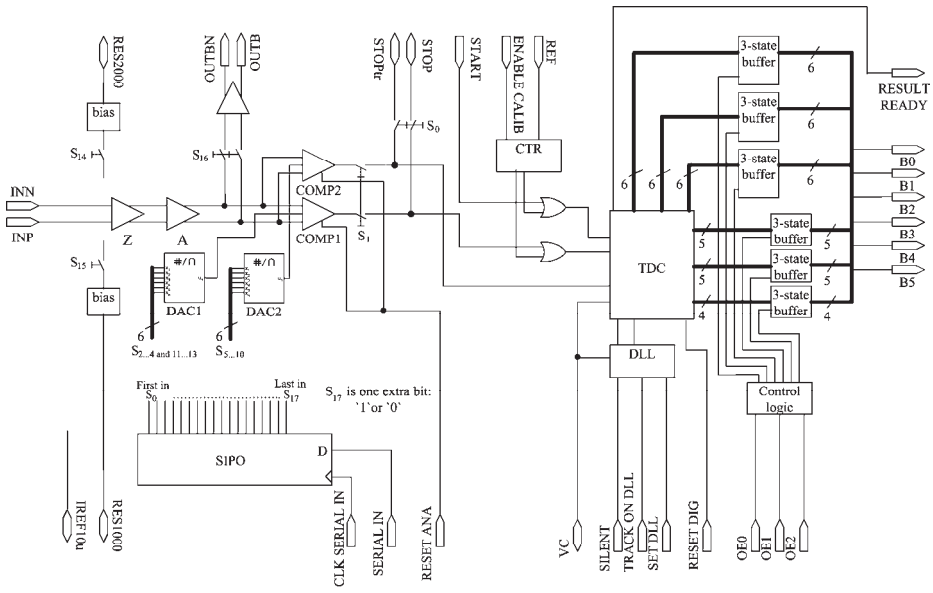


**Fig. 18. Block diagram of the receiver chip with I/O connection (VI, published by permission of IEEE).**

## 6.1 Structure and operation of the receiver channel

A simplified block diagram of the receiver channel is shown in Fig. 19, where a single-ended receiver channel is shown for clarity instead of the fully differential structure that was used in the final realization. It also shows connections to the TDC, even though the designing of the TDC lies beyond the scope of this thesis. The receiver channel consists of a fully differential transimpedance preamplifier, a postamplifier and two identical timing comparators. The thresholds of the two comparators can be adjusted independently by means of two identical on-chip DACs, shown in Fig. 18, so that different threshold setups can be investigated.

Operation of the receiver channels is as follows. The current signal from the APD is first amplified by the preamplifier and further amplified by the postamplifier. The voltage signal from the postamplifier is fed to the two identical timing comparators with different thresholds, which give logic-level timing marks for the TDC. The timing delay between the comparator outputs is proportional to the signal amplitude and can be measured by the TDC. In other words, the TDC measures the time interval between the START and STOP signals shown in Fig.

19, which corresponds to the actual flight time from the transmitter to the target and back to the receiver, and additionally the time interval between the STOP and STOPtr signals, a threshold time interval Δt which is proportional to the signal amplitude, in which case the latter time interval can be used to compensate for the walk error.

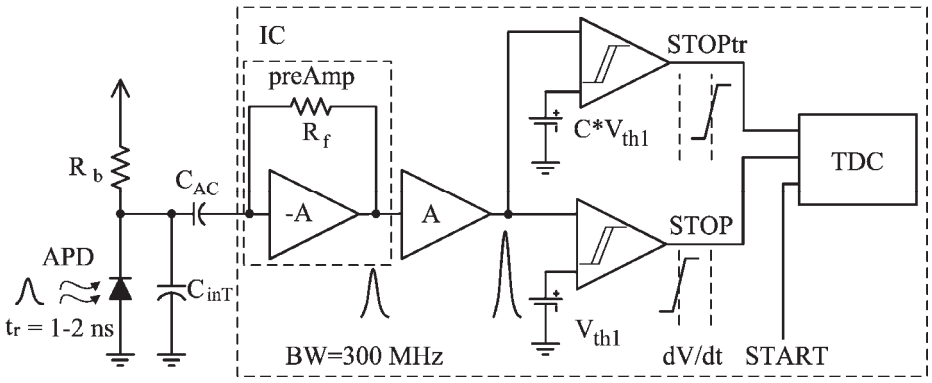


**Fig. 19. Block diagram of the receiver channel (VI, published by permission of IEEE).**

The threshold settings are important, because they affect aspects of the achievable performance such as the dynamic range, the minimum detectable signal and the single-shot precision. To avoid false detection on account of noise, the lower threshold should correspond to at least an SNR of 10 (peak signal vs. rms noise), in which case the higher threshold can be chosen to be around an SNR of 20, for example. Thus the minimum detectable walk-compensated signal would correspond to approximately an SNR of 20. To achieve as wide a dynamic range as possible, the higher threshold should be chosen to be as low as possible, bearing in mind, however, that the single-shot precision starts to deteriorate as the ratio between the thresholds decreases, as explained in Section 3.3.2. Thus an SNR of 20 was chosen as the threshold for the second comparator. At a higher signal level a higher threshold can also be used for the second comparator to improve the single-shot precision.

## 6.2 Measurement results

A photograph of the receiver ASIC of the pulsed TOF rangefinder is shown in Fig. 20. The size of the layout, including the TDC and pad ring, was 1300 µm × 1300

μm and the power consumption of the receiver channel was 30 mW. Before any measurements were made with the receiver channel, the performance of the TDC was assessed by using logical timing signals generated by the pulse generator. The single-shot precision of the TDC was better than 20 ps at time intervals from zero to 100 ns and its accuracy was ±5 ps over a range from 5 ns to 100 ns (Nissinen I & Kostamovaara 2009). The compensation curve was also defined first by measuring the timing walk as a function of the threshold time interval Δt. This calibration of the receiver is probably not necessarily needed for every circuit, depending, of course, on the accuracy required.

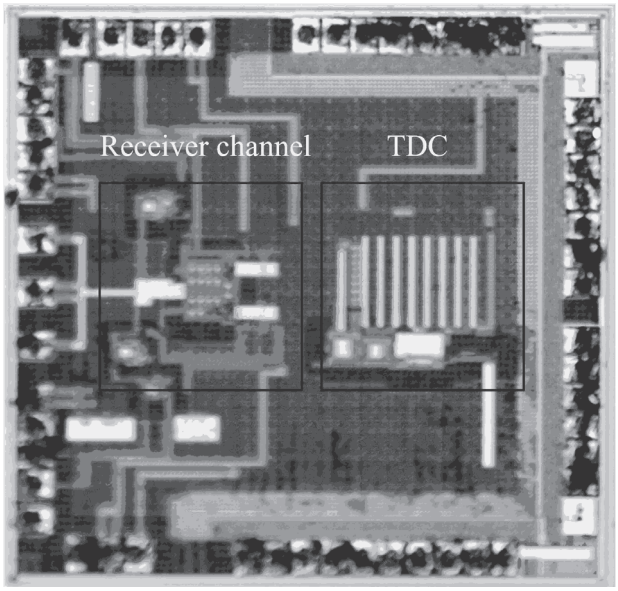


**Fig. 20. Photograph of the receiver chip fabricated in a 0.13μm CMOS process (VI, published by permission of IEEE).**

Measurements of two kinds were carried out to determine the achievable performance. Firstly the receiver channel was measured by using a pulse generator to generate the electrical start signal for the TDC and the delayed triggering signal for the laser pulser which transmits an optical laser pulse to the receiver. An optical neutral density filter was used between the transmitter and the receiver to attenuate the power of the optical stop pulse within a range that covered the whole required dynamic range of the receiver channel. The

measurement results are given in Section 6.2.1. Secondly, the receiver chip was inserted into a pulsed TOF laser rangefinder and actual distance measurements were made to prove its functionality in the application environment. These results are given in Section 6.2.2.

### *6.2.1 Measurements using the optical neutral density filter*

The rise time of the optical pulse was shown in Papers VII and VIII to be approximately 3 ns, and the measurements obtained using that laser pulse are discussed in those papers. According to Section 3.1.1, the rise time of the optical pulse should be 0.35/BW to achieve the best jitter properties. Thus an optical pulse with a rise time of 1.5 ns, which is close enough to the measured bandwidth of 300 MHz, was also used, the measurements obtained with which are presented in this chapter. Before these measurements were made the compensation curve was first determined by varying the amplitude of the optical pulse over a dynamic range of 1:10 000 and collecting the results regarding the threshold time interval $\Delta t$ and the timing walk at specific amplitudes. Two threshold settings for the comparators were used, SNRs of 10 and 20 and SNRs of 10 and 30, to ascertain the effect of the threshold settings on the achievable accuracy, single-shot precision and dynamic range. Compensation curves measured with both sets of threshold settings are shown in Fig. 21.

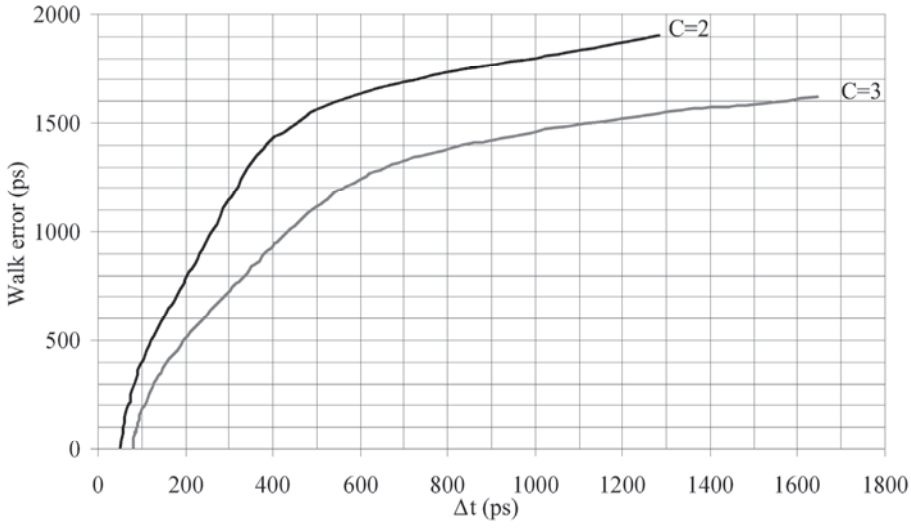


**Fig. 21. Compensation curves with C values of two (black) and three (grey).**

The accuracy of the timing detection was measured by averaging 5000 measurements at every amplitude within a dynamic range of 1:10 000, which implies an amplitude domain from 2 μA to 20 mA with a C value of two and from 3 μA to 30 mA with a C value of three, and compensating for the walk error by using the averaged threshold time interval Δt results and the compensation curve. The walk error after compensation, shown as a function of the measured threshold time interval Δt with C values of two (grey) and three (black) in Fig. 22, was approximately ±25 ps with a C value of two and ±20 ps with C value of three within a dynamic range of 1:10 000.

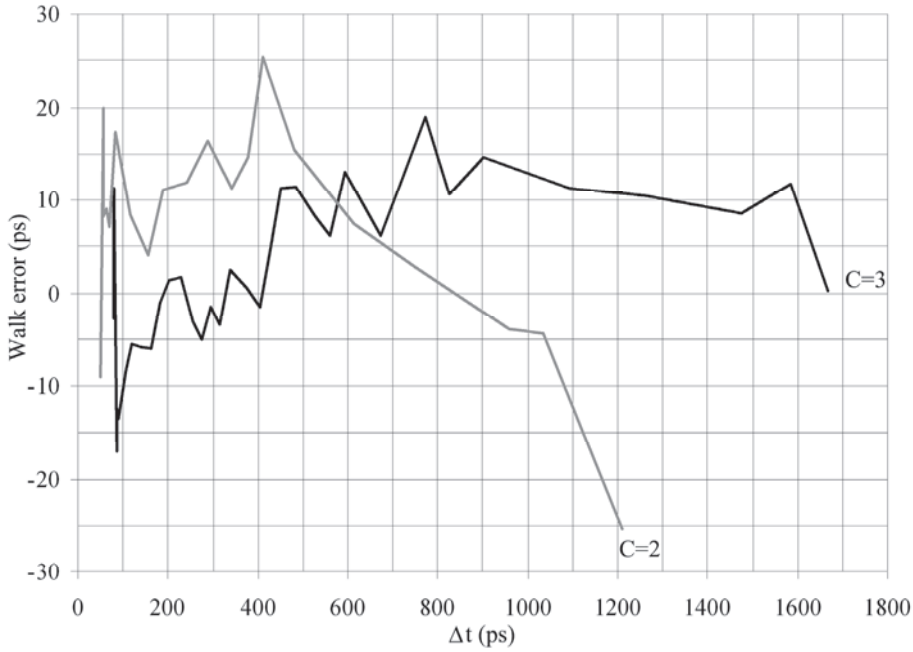


**Fig. 22. Compensated walk error with a C value of three (black) and a C value of two (grey).**

The single-shot precision of the receiver channel was measured by sweeping the amplitude of the pulse over a dynamic range of 1:10000 and making 5000 measurements at each amplitude. Two threshold setups were used to confirm the impact of the larger threshold ratio on the single-shot precision, as explained in Section 3.3.2. To see how the compensation affects the single-shot precision of the final measurement result, compensation was first performed on each of the 5000 samples separately so that they were treated as individual single-shot measurements. After that the standard deviation of the compensated result were calculated at the each amplitude. The standard deviations of the compensated results and of the actual measurement results at the lower threshold (time difference between START and STOP) are shown as a function of the measured threshold time interval Δt with C values of two (grey line) and three (black line) in Fig. 23. As can be seen, the standard deviation of the compensated results starts to deteriorate at higher signal levels (Δt ~600 ps with C = 2 and 800 ps with C = 3)

on account of the deeper slope of the compensation curve (Fig. 21). On the other hand, the slope of the compensation curve remains constant from 400 ps with C = 2 and 500 ps with C = 3 down to approximately 100 ps, and thus the progressively smaller jitter of the measured threshold time interval Δt finally starts to improve the single-shot precision, until it starts to deteriorate again because of the deeper slope of the compensation curve around 100 ps caused by slew rate limitation of the comparator, as explained in Section 3.3.2. The same information is presented as a function of signal amplitude in Fig. 24.

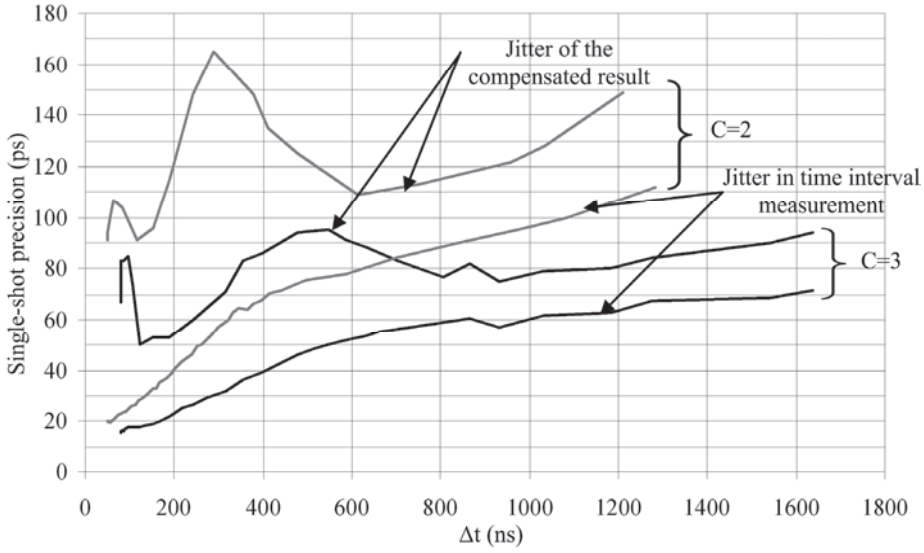


**Fig. 23. Single-shot precision of the compensated results with C values of two (grey) and three (black) and jitter in the actual time interval measurements.**

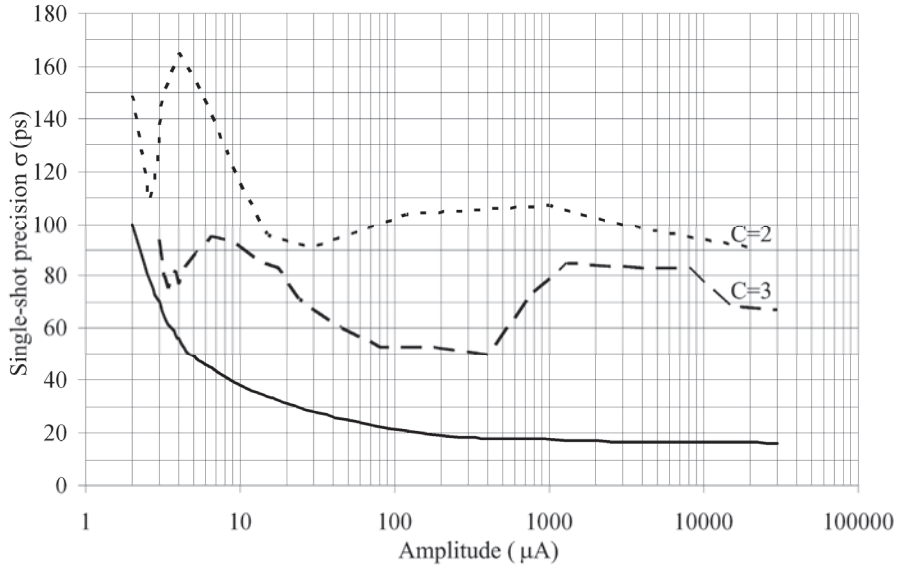


**Fig. 24. Measured single-shot precision with C values of two (dotted line) and three (dashed line) and jitter at the lower threshold (solid line).**

### *6.2.2 Time-of-flight laser rangefinding*

Actual distance measurements were carried out using a calibrated measurement track where the distance from the target can be adjusted by computer. A measurement head with transmitter and receiver optics was used to collimate the laser beam, and graded index optical fibres were used to conduct the optical signal from the semiconductor laser to the measurement head and from the measurement head to the APD. The electrical start pulse was generated by conducting a small portion of the transmitted optical signal to the receiver channel, which was fabricated from discrete components. A comparator at the output of the discrete receiver channel produced the logic level start signal for the TDC. At the beginning the compensation curve was defined by measuring the flight time from the transmitter to a target at a constant distance and back to the receiver and by varying the amplitude of the optical signal with a neutral density filter. The reflectance of the surface of the target was also altered to cover the whole dynamic range of the receiver.

In the linearity measurements the distance from the target was swept from one metre to 21 m with 0.5 metre steps when using a sheet of white paper as the target and one metre steps with a diamond-grade reflective sheet as the target. The reflected optical power varied by more than 1:2000 in this setup, due both to the difference in reflectance properties between the white paper and the reflective sheet and to the distance variation. The distance measurement accuracy as a function of the distance from the target is shown separately for the white paper (black line) and the diamond-grade reflective sheet (grey line) in Fig. 25. Each point on the curves corresponds to a deviation in the measured distance from the actual distance. The accuracy is better than ± 5 mm at distances from 4 metres to 21 metres, the peaks at a distance of ~2 metres, being due to disturbance from the optical start pulse, as the comparator at the output of the discrete start channel changes state at both the rising and falling edges of the optical pulse. The falling edge causes disturbance in the measurements at a time interval that corresponds to the widths of the optical pulse. This can be avoided by using a latch as the output stage, but this was not possible with the measurement setup used here.

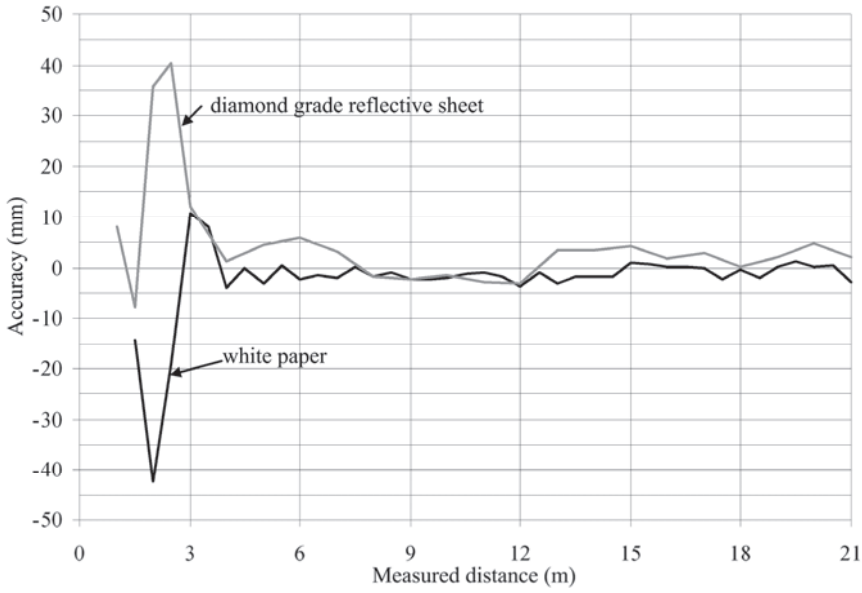


**Fig. 25. Nonlinearity of the distance measurement with white paper (black line) and a diamond-grade reflective sheet (grey line) as the targets, total amplitude variation > 1:2000.**

# 7 Discussion

The purpose of this overall project has been to study and develop CMOS receiver channels for pulsed time-of-flight laser rangefinding, with special attention paid to preamplifiers, postamplifiers and timing comparators. As far as the receiver channel is concerned the main target has been to achieve as small a timing error as possible with as wide a dynamic range and as a simple structure as possible. Several receiver channel structures are proposed in this thesis that meet such requirements. Receiver channels using both linear mode and leading edge timing discrimination are considered and methods are proposed for compensating for walk error. In particular, a new time domain walk error compensation principle is presented.

The main goal of this work was to fabricate a CMOS receiver channel for a laser radar receiver chip which would also include an on-chip TDC. A receiver chip of this kind would be useful for increasing the level of integration of the whole pulsed TOF laser rangefinder, and it would also help to reduce the size and complexity of the laser radar device, which would be beneficial in proximity switch applications, for example. Another aim was to fabricate an integrated semiconductor laser driver in a CMOS technology which would also help to achieve smaller size and reduce the complexity of the whole laser radar.

Some laser radar applications demand a large dynamic range of at least 1:10 000…100 000 or even more, which calls for a receiver channel which can produce an accurate timing moment from the received pulse even though it may be saturated in the amplitude domain. This eventually leads to the use of a leading edge timing discriminator, because the lack of linear range in modern IC technologies caused by the low power supply voltage. A new compensation principle is proposed in this thesis for correcting the timing error in the leading edge timing discriminator by using the TDC to measure the slew rate of the leading edge of the pulse and to performing the compensation on the basis of the resulting data. In a sense the proposed compensation technique can be seen as a time-domain AD conversion in which the strength of the pulse is evaluated in the time domain and not in the amplitude domain, where the voltage headroom of the receiver channel would limit the dynamic range of the compensation. The principle also benefits from the fact that the TDC already exists in the system and only needs an extra channel to perform the compensation. The performance of the receiver channel fabricated in a 0.13 μm CMOS technology was also

demonstrated in a real laser ranging environment by using an optical measurement head and a calibrated measurement track.

The integration of a CMOS semiconductor laser diode driver was also investigated to test the possibility of using this to generate an ampere-scale current pulse through low ohmic loads. The performance of the laser diode driver fabricated in a 0.35 µm CMOS technology was measured using ohmic loads and a semiconductor laser diode load. To the author's knowledge there is only one other paper concerning an integrated CMOS laser driver (Wens *et al.* 2009), and it was actually published in the autumn of the same year as Paper VIII. Wens *et al.* used a special high voltage 0.35 µm CMOS technology and achieved a 10 A current pulse with the rise time of 2.2 ns. The proposed pulser used three supply voltages: 3.3 V, 12 V and 70 V. By comparison, our design, realized in a 0.35 µm CMOS technology, had a peak current pulse, a rise time and supply voltages of 1 A, 900 ps and 3.3 V and 5 V, respectively.

In the field of timing discriminators several methods have been published for avoiding walk error and achieving as wide a dynamic range as possible. Palojärvi *et al.* (2005) reported ±35 mm accuracy within a dynamic range of 1:4000 in a 0.8 µm BiCMOS process, and Kurtti & Kostamovaara (2011) reported ±2.3 mm accuracy within a dynamic range of 1:100 000 in a 0.35 µm BiCMOS process. Both receivers use a leading edge timing discriminator, and in addition the former used the amplitude information to correct the walk error. The latter measured the width of the received pulse and used the resulting data to compensate for the walk error. In the field of radiation detectors, Despeisse *et al.* (2009) fabricated a timing discriminator which also used pulse width information to correct the timing error within a dynamic range of 1:10 and achieved timing jitters of 175 ps and 25 ps with a LCO (Low Capacitance and consumption Optimization) circuit and a HCO (High Capacitance Optimization) circuit, respectively. The leading edge timing discriminators presented in Papers VI and I achieved ±4.5 mm within a dynamic range of 1:10000 and ±45 mm within a dynamic range of 1:1000, respectively, using optical pulses of width approximately 3 ns and 6 ns, respectively. Currently existing results regarding leading edge timing discriminators are summarized in Table 1.

**Table 1. Results of studies on leading edge timing discriminators.**

| Discriminator | Walk error | Jitter | Dynamic range | Process | Reference |
|---|---|---|---|---|---|
| Leading edge + peak detector | ±35 mm | <9.5 mm @ SNR>35 | 1:4000 | 0.8 μm BiCMOS | Palojärvi *et al.* (2005) |
| Leading edge + pulse width measurement | ±2.3 mm | <18 mm @ SNR>10 | 1:100 000 | 0.35 μm BiCMOS | Kurtti & Kostamovaara (2010) |
| Leading edge + pulse width measurement | NA | 26 mm(LCO) 3.8 mm(HCO) | 1:10 | 0.13 μm CMOS | Despeisse *et al.* (2009) |
| Leading edge + slew rate measurement | ±4.5 mm[a] ±3.8 mm[b] | <37.5 mm @ SNR > 20[a] | 1:10 000 | 0.13 μm CMOS | Paper VI |
| Leading edge + two peak detectors | ±45 mm | NA | 1:1000 | 0.35 μm CMOS | Paper I |

[a] with rise time of 3 ns, [b] with rise time of 1.5 ns

A receiver channel fabricated in a 0.8 μm BiCMOS process and based on a linear timing discriminator with gain control has been reported to achieve ±4.7 mm accuracy within a dynamic range of 1:624 (Ruotsalainen *et al.* 2001), while Kurtti & Kostamovaara (2009a) and Pehkonen *et al.* (2006) have proposed a linear timing discriminator scheme without gain control in which accuracies of ±8 mm and ±5.6 mm were achieved within dynamic ranges of 1:3000 and 1:1280, respectively. Both receiver channels had been fabricated in a 0.35 μm BiCMOS technology. Simpson *et al.* (1997) have also proposed a time interval measurement system for the WA-98 calorimeter which uses a C-R differentiator to produce an amplitude-independent timing moment and have achieved a total accuracy of ±250 ps, equivalent to ±37.5 mm, within a dynamic range of 1:100 with a pulse that had a rise time of 10 ns. They have also integrated a time interval measurement unit based on a time-to-amplitude converter onto the same chip.

The two receiver channels proposed in Paper III achieved simulated timing accuracies of ±6.8 mm and ±7 mm within dynamic ranges of 1:1600 and 1:1200, respectively. The performance of linear timing discriminators as published to date is summarized in Table 2.

**Table 2. Results of studies on linear timing discriminators.**

| Discriminator | Walk error | Jitter | Dynamic range | Process | Reference |
|---|---|---|---|---|---|
| High-pass with gain control | ±4.7 mm | <36 mm @SNR>20 | 1:624 | 0.8μm BiCMOS | Ruotsalainen *et al.* (2001) |
| High-pass after current buffer | ±8 mm | <37 mm @SNR>20 | 1:2750 | 0.35μm BiCMOS | Kurtti & Kostamovaara (2009a) |
| RLC resonance-based | ±5.6 mm | <33 mm @SNR>10 | 1:1280 | 0.35μm BiCMOS | Pehkonen *et al.* (2006) |
| High-pass | ±37.5 mm | 32 mm at the maximum | 1:100 | 1.2 μm CMOS | Simpson *et al.* (1997) |
| High-pass at input and after current buffer | ±6.8 mm<br>±7 mm | NA<br>NA | 1:1600<br>1:1200 | 0.18 μm CMOS<br>0.18 μm CMOS | Paper III |

To the best of the author's knowledge, there are only a few papers describing receiver chips which include both the receiver channel and the time interval measurement unit for a pulsed time-of-flight rangefinder. Paschalidis *et al.* (2002) reported an on-chip time-of-flight system, but this used a photomultiplier as the detector. They achieved a 350 ps timing walk for an input amplitude dynamic range of 1:100 and a single-shot precision of 180 ps. Copani *et al.* (2008) presented a fully integrated time-of-flight measurement system and achieved 12 ps resolution, but their paper does not contain any other information on time-of-flight measurements. Palojärvi *et al.* (2001) reported ±12 mm nonlinearity over a measurement range from 0.3 m to 22 m and a single-shot precision of 51 mm with an SNR of 11. The chip included four integrated photodiodes, receiver channels and a four-channel TDC and had been fabricated in a 0.8 μm BiCMOS technology. The dynamic range of the receiver channels was only 1:20, however. Delaye & Labeye (2000) proposed a totally different principle for achieving an accurate timing event based on a fast digitizer with an acquisition rate of 10 GS/s reported a distance accuracy of ±5 mm within a dynamic range of 1:20. The receiver was constructed from discrete components and acquisition took place through a digital oscilloscope. The receiver chip reported in Paper VI achieved a nonlinearity of ±5 mm over a distance range from 4 m to 21 m and a single-shot precision of less than 100 ps (σ-value), equivalent to 15 mm in distance, with an SNR of at least 30. The dynamic range of the receiver channel was 1:10 000.

# 8 Summary

There is potentially a huge market for pulsed TOF laser radar technology having high level of integration in order to keep the fabrication costs low. Perception systems in the automotive and robot industries, for example, could very well make use of such devices. Thus the general goal of the present work was to fabricate a receiver chip for a pulsed time-of-flight laser rangefinder which would include both the receiver channel and the TDC on a single die. It was believed that in this way the integration level of the whole laser radar could be increased and thus laser radars of smaller size and costs could be manufactured. Regarding receiver channels, which form the main topic of the present thesis, the aim was to design these in CMOS technologies so that they could generate an accurate timing moment despite the large variation in the amplitude of the received pulse. In addition, the feasibility of a CMOS semiconductor laser diode driver was demonstrated. Both of these goals will pave the way to the construction of a compact pulsed time-of-flight micromodule.

The purpose of the receiver channel is to produce a logic-level timing mark for the TDC from the widely varying current signal produced by the photodetector. Because of the great variation in the amplitude of the received optical signal, which may exceed 1:10 000, a systematic timing error in the nanosecond range occurs with the pulse width that is normally used, which is of the order of a few nanoseconds. Another error source in the timing discriminator is noise, which introduces timing jitter into the measurements. Thus in order to minimize the error sources, special timing discrimination schemes or compensation procedures have to be used and the noise of the receiver has to be minimized.

Four receiver channels were designed in the course of the present work, including two with a leading edge timing discriminator, the first of which uses information on the amplitude of the received pulse to compensate for the timing error, while the second measures the slew rate of the received pulse and uses this information to compensate for the timing error. The compensated walk errors of channels of the first and second types were ±45 mm within a dynamic range of more than 1:1000 and ±3.8 mm within a dynamic range of more than 1:10 000, when the pulse widths were approximately 6 ns and 3 ns, respectively. The other two receiver channels were based on a linear timing discrimination scheme and achieved a simulated accuracy of ±9 mm within a dynamic range of more than 1:1000.

A CMOS semiconductor laser diode driver was shown to generate an ampere-scale current pulse through a low ohmic load with a power supply of only 5 V. With this peak current an optical power of about 500 mW was achievable from a semiconductor laser diode. If higher power levels are needed, special high-voltage CMOS technologies can be used with the proposed pulser scheme to obtain the higher pulse current needed.

The results presented in this thesis show that leading edge detection with time domain walk compensation is a potential solution to the problem of a restricted linear range that affects modern CMOS technology. Because of the large walk error that occurs in basic leading edge detection methods, compensation techniques have to be used to achieve as wide a dynamic range and as small a walk error as possible. One potential future compensation method in addition to that based on slew-rate measurements proposed here could be the use of a combination of time domain compensation methods. Measuring both the slew-rate and the width of the pulse could be an interesting combination, for example. Both compensation methods benefit from the fact that the TDC is already available on the chip and needs only a small modification to perform the compensation.

# References


Abidi AA (1987) On the noise optimum of gigahertz FET transimpedance amplifier. IEEE Journal of Solid-State Circuits 22(6): 1207–1209.

Ahola R (1979) Design of the transmitter and receiver of a laser rangefinder system for moving targets. MSc thesis, University of Oulu, Department of Electrical Engineering.

Araki T & Yoshido H (1996) Optical distance meter using a pulse laser diode and fast avalanche photo diode for measurements of molten steel levels. ASME Journal of Dynamic Systems, Measurement, and Control 118: 800–803.

Arbel A. (1980) Analog signal processing and instrumentation. Cambridge, Cambridge University Press.

Baker RJ & Pocha MD (1990) Nanosecond switching using power MOSFETs. Rev Sci Instrum 61(8): 2211–2213.

Bertolini G (1968) Pulse shape and time resolution. In: Bertolini G & Coche A (eds) Semiconductor detectors. Amsterdam, North-Holland Publishing.

Copani T, Vermeire B, Jain A, Karaki H, Chandrashekar K, Goswami S, Kitchen J, Chung H. H, Deligoz I, Bakkaloglu B, Barnaby H & Kiaei S (2008) A Fully Integrated Pulsed-laser Time-of-Flight Measurement Sytem with 12 ps Single-Shot Precision. Proc. IEEE Custom Integrated Circuits Conference, San Jose, California, USA: 359–362.

Despeisse M, Jarron P, Anghinolfi F, Tiuraniemi S, Osmic F, Riedler P, Kluge A and Ceccucci A (2009) Low-Power Amplifier-Discriminators for High Time Resolution Detection. IEEE Transactions on Nuclear Science 56(2): 375–381.

Gedcke DA & McDonald WJ (1967) A constant fraction of pulse height trigger for optimum time resolution. Nuclear Instruments and Methods 55: 377–380.

Gedcke DA & Williams CW (1968) High resolution time spectroscopy. Ortec Application note No.1.

Goldstein BS & Dalrymble GF (1967) Gallium arsenide injection laser radar. Proc IEEE 55(2): 181–188.

Hewlett Packard Inc. Time interval averaging. Application Note 162–1.

Howard L & Daneshvar K (1989) Nanosecond-pulse generator for laser diodes. Rev Sci Instrum 60(10): 3343–3345.

Ingels M & Steyaert MSJ (1999) A 1-Gb/s, 0.7-μm CMOS optical receiver with full rail-to-rail output swing. IEEE Journal of Solid-State Circuits 34(7): 971–977.

Kaisto I, Kostamovaara J, Manninen M & Myllylä R (1993) Laser radar-based measured system for large scale assembly applications. Proc SPIE International Conference on Laser Dimensional Metrology: Recent Advances for Industrial Application, Brighton, United Kingdom, 2088: 121–130.

Kawashima S, Watanabe K & Kobayashi K (1995) Traffic condition monitoring by laser radar for advanced safety driving. Proceedings of the Intelligent Vehicles 1995 Symposium, Detroit, USA: 299–303.

Kilpelä A & Kostamovaara J (1997) Laser pulser for a time-of-flight laser radar. Rev Sci Instrum 68(6): 2253–2258.

Kostamovaara J, Määttä K, Koskinen M & Myllylä R (1992) Pulsed Laser Radars with High-Modulation-Frequency in Industrial Applications. Proc SPIE conference on Laser Radar VII: Advanced Technology for applications, Los Angeles, California, USA, 1633: 114–127.

Kurtti S & Kostamovaara J (2005) An integrated optical receiver with wide-range timing discrimination characteristics. Proceedings of the 31st European solid-state circuits conference, Grenoble, France: 435–438.

Kurtti S & Kostamovaara J (2009a) Laser Radar Receiver Channel With Timing Detector Based on Front End Unipolar-to-Bipolar Pulse Shaping. IEEE Journal of Solid-State Circuits 44(3): 835–847.

Kurtti S & Kostamovaara J (2009b) Pulse width time walk compensation method for a pulsed time-of-flight laser rangefinder. IEEE International Instrumentation and Measurement Technology Conference, Singapore: 1059–1062.

Kurtti S & Kostamovaara J (2011) An integrated laser radar receiver channel utilizing a time-domain walk error compensation scheme. IEEE Transaction on Instrumentation and Measurement 60(1): 146–157.

Lim H & Park J (2003) Comparison of time corrections using charge amouts, peak values, slew rates, and signal widths in leading-edge discriminators. Review of Scientific Instruments 74(6): 3115–3119.

Määttä K, Kostamovaara J & Myllylä R (1993) Profiling of hot surfaces by pulsed time-of-flight laser range finder techniques. Applied Optics 32(27): 5334–5347.

Määttä K (1995) Pulsed time-of-flight laser rangefinding techniques and devices for hot surface profiling and other industrial application. Acta Univ Oulu C 81.

Ng TC, Guzmán JI & Tan JC (2004) Development of a 3D LADAR system for autonomous navigation. Proc IEEE Conference on Robotics, Automation and Mechatronics, Singapore, 2: 792–797.

Nissinen I, Mäntyniemi A & Kostamovaara J (2003) A CMOS time-to-digital converter based on a ring oscillator. Proceedings of the 29th European solid-state circuits conference, Estoril, Portugal: 469–472.

Nissinen I & Kostamovaara J (2009) A 2-channel CMOS time-to-digital converter for time-of-flight laser rangefinding. IEEE Instrumentation and Measurement Technology Conference, Singapore: 1647–1651.

Palojärvi P, Mäntyniemi A & Kostamovaara J (2001) A Multi-channel Pulsed Time-of-Flight Laser Radar Chip. Proceedings of ODIMAP III 3rd Topical Meeting on Optoelectronic Distance Measurement and Applications, Pavia, Italy: 112–117.

Palojärvi P, Ruotsalainen T & Kostamovaara J (2002) Pulsed Time-of-Flight Laser Radar Module with mm-level Accuracy Using Full Custom Receiver and TDC ASICs. IEEE Transaction on Instrumentation and Measurement 51(5): 1102–1108.

Palojärvi P (2003) Integrated electronic and optoelectronic circuits and devices for pulsed time-of-flight laser rangefinding. Acta Univ Oulu C 181.

Palojärvi P, Ruotsalainen T & Kostamovaara J (2005) A 250-MHz BiCMOS receiver channel with leading edge timing discriminator for a pulsed time-of-flight laser rangefinder. IEEE Journal of Solid-State Circuits 40(6): 1341–1349.

Pananurak W, Thanok S & Parnichkun M (2008) Adaptive Cruise Control for an Intelligent Vehicle. Proc IEEE International Conference on Robotics and Biomimetics, Bangkok, Thailand: 1794–1799.

Park SM & Toumazou C (1998) Low noise current-mode CMOS transimpedance amplifier for giga-bit optical communication. Proceedings of the IEEE International Symposium on Circuits and Systems, Monterey CA, USA: 293–296.

Park SM & Yoo H-J (2004) 1.25-Gb/s regulated cascode CMOS transimpedance amplifier for gigabit ethernet application. IEEE Journal of Solid-State circuits 39(1): 112–121.

Paschalidis N, Stamatopoulos N, Karadamoglou K, Kottaras G, Paschalidis V, Sarris E, McNutt R, Mitchell D & McEntire R (2002) A CMOS Time-of-Flight System-on-a-Chip for Spacecraft Instruments. IEEE Transactions on Nuclear Science 49(3): 1156–1163.

Pehkonen J & Kostamovaara J (2003) Walk error minimization by resonance-based laser pulse timing detection. Electronics Letters 39(23): 1624–1625.

Pehkonen J, Palojärvi P & Kostamovaara J (2006) Receiver channel with resonance-based timing detection for a laser range finder. IEEE Transactions on Circuits and systems I: Regular Papers 53(3): 569–577.

Peltola T, Ruotsalainen T, Palojärvi P & Kostamovaara J (2000) A receiver channel with a leading edge timing discriminator for a pulsed time-of-flight laser radar. Proceedings of the 26th European solid-state circuits conference, Stockholm, Sweden: 428–431.

RCA Corporation (1974) RCA Electro-Optics Handbook, RCA, Inc., Lancaster Pa., tech. ser. EOH-11.

Ruotsalainen T, Palojärvi P & Kostamovaara J (1999a) A Current-mode gain-control scheme with constant bandwidth and propagation delay for a transimpedance preamplifier. IEEE Journal of Solid-State circuits 34(2): 253–258.

Ruotsalainen T (1999b) Integrated receiver channel circuits and structures for a pulsed time-of-flight laser radar. Acta Univ Oulu C 136.

Ruotsalainen T, Palojärvi P & Kostamovaara J (2001) A wide dynamic range receiver channel for a pulsed time-of-flight laser radar. IEEE Journal of Solid-State circuits 36(8): 1228–1238.

Räisänen-Ruotsalainen E, Rahkonen T & Kostamovaara J (2000) An Integrated Time-to-Digital Converter with 30-ps Single-Shot Precision. IEEE Journal of Solid-State circuits 35(10): 1507–1510.

Simpson ML, Britton CL, Wintenberg AL & Young GR (1995) An integrated, CMOS, constant-fraction timing discriminator for multichannel detector systems. IEEE Transaction on Nuclear Science 42(4): 762–766.

Simpson ML, Britton CL, Wintenberg AL & Young GR (1997) An Integrated CMOS Time Interval Measurement System with Subnanosecond Resolution for the WA-98 Calorimeter. IEEE Journal of Solid-State circuits 32(2): 198–205.

Simpson ML & Paulus MJ (1998) Discriminator Design Consideration for Time-Interval Measurement Circuits in Collider Detector Systems. IEEE Transaction on Nuclear Science 45(1): 98–104.

Säckinger E (2005) Broadband circuits for optical fiber communication. Hoboken NJ, Wiley.

Thompson MT & Schlecht MF (1997) High Power Laser Diode Driver Based on Power Converter technology. IEEE Transactions on Power Electronics 12(1): 46–52.

Tsuchiya Y, Takeshima A & Hosoda M (1981) Stable ultrashort laser diode pulse generator. Rev Sci Instrum 52(4): 579–581.

van de Plassche R & Baltus P (1988) An 8-bit 100 MHz Full-Nyquist Analog-to-digital Converter. IEEE Journal of Solid-State Circuits 23(6): 1334–1344.

van de Plassche R (1994) Integrated analog-to-digital and digital-to-analog converters. Dordrecht, Kluwer Academic Publisher.

Velupillai S & Guvenc L (2009) Laser Scanners for Driver-Assistance Systems in Intelligent Vehicles. IEEE Control Systems Magazine 29(2): 17–19.

Wens M, Redouté J-M, Blanchaert T, Bleyaert N & Steyaert M (2009) An Integrated 10A, 2.2ns Rise-Time Laser-Diode Driver for LIDAR Applications. Proceedings of the 35th European solid-state circuits conference, Athens, Greece: 144–147.

Ziemer RE & Tranter WH (1985) Principles of communications systems, modulation and noise. Boston, Houghton Mifflin Company.

# Original publications

I Nissinen J, Palojärvi P & Kostamovaara J (2003) A CMOS Receiver for a Pulsed Time-of-Flight Laser Rangefinder. Proceedings of the IEEE European Solid-State Circuits Conference (ESSCIRC'2003). Estoril, Portugal, 16–18 Sep. 2003: 325–328.©

II Nissinen J, Nissinen I, Palojärvi P, Mäntyniemi A & Kostamovaara J (2004) A CMOS Receiver Chip Consisting of a Receiver Channel and Time-to-Digital Converter for a Laser Radar. Proceedings of the 4th Topical Meeting on Optoelectronic Distance Measurement and Applications (ODIMAP'2004). Oulu, Finland, 16–18 June 2004: 164–169.

III Nissinen J & Kostamovaara J (2004) Wide Dynamic Range CMOS Receivers for a Pulsed Time-of-Flight Laser Range Finder. Proceedings of the IEEE Instrumentation and Measurement Technology Conference (IMTC'2004). Como, Italy, 18–20 May 2004, 2: 1224–1227.

IV Nissinen J & Kostamovaara J (2006) Fully Differential, Regulated Cascode Amplifier. Proceedings of the IEEE Mediterranean Electrotechnical Conference (MELECON'2006). Benalmadena, Spain, 16–19 May 2006: 51–54.

V Nissinen J & Kostamovaara J (2007) An Integrated Laser Radar Receiver Channel with Wide Dynamic Range. Proceedings of the IEEE International Conference on Electronics, Circuits and Systems (ICECS'2007). Marrakech, Morocco, 17–18 Dec. 2007: 10–13.

VI Nissinen J, Nissinen I & Kostamovaara J (2009) Integrated receiver including both receiver channel and TDC for a pulsed time-of-flight laser rangefinder with cm-level accuracy. IEEE Journal of Solid-State Circuits 44(5): 1486–1497.

VII Nissinen J & Kostamovaara J (2009) A 0.13 µm CMOS Laser Radar Receiver with Leading Edge Detection and Time Domain Error Compensation. Proceedings of the IEEE International Instrumentation and Measurement Technology Conference (I2MTC'2009). Singapore, 5–7 May 2009: 900–903.

VIII Nissinen J & Kostamovaara J (2009) A 1 A laser driver in 0.35 µm complementary metal oxide semiconductor technology for a pulsed time-of-flight laser rangefinder. Review of Scientific Instruments 80(10): 104703.



Original publications are not included in the electronic version of the dissertation.

373. Lee, Young-Dong (2010) Wireless vital signs monitoring system for ubiquitous healthcare with practical tests and reliability analysis

374. Sillanpää, Ilkka (2010) Supply chain performance measurement in the manufacturing industry : a single case study research to develop a supply chain performance measurement framework

375. Marttila, Hannu (2010) Managing erosion, sediment transport and water quality in drained peatland catchments

376. Honkanen, Seppo (2011) Tekniikan ylioppilaiden valmistumiseen johtavien opintopolkujen mallintaminen — perusteena lukiossa ja opiskelun alkuvaiheessa saavutettu opintomenestys

377. Malinen, Ilkka (2010) Improving the robustness with modified bounded homotopies and problem-tailored solving procedures

378. Yang, Dayou (2011) Optimisation of product change process and demand-supply chain in high tech environment

379. Kalliokoski, Juha (2011) Models of filtration curve as a part of pulp drainage analyzers

380. Myllylä, Markus (2011) Detection algorithms and architectures for wireless spatial multiplexing in MIMO-OFDM systems

381. Muhos, Matti (2011) Early stages of technology intensive companies

382. Laitinen, Ossi (2011) Utilisation of tube flow fractionation in fibre and particle analysis

383. Lasanen, Kimmo (2011) Integrated analogue CMOS circuits and structures for heart rate detectors and other low-voltage, low-power applications

384. Herrala, Maila (2011) Governance of infrastructure networks : development avenues for the Finnish water and sewage sector

385. Kortelainen, Jukka (2011) EEG-based depth of anesthesia measurement : separating the effects of propofol and remifentanil

386. Turunen, Helka (2011) $CO_2$-balance in the athmosphere and $CO_2$-utilisation : an engineering approach

387. Juha, Karjalainen (2011) Broadband single carrier multi-antenna communications with frequency domain turbo equalization

388. Martin, David Charles (2011) Selected heat conduction problems in thermomechanical treatment of steel

Book orders:
Granum: Virtual book store
http://granum.uta.fi/granum/

UNIVERSITY OF OULU P.O.B. 7500 FI-90014 UNIVERSITY OF OULU FINLAND

# ACTA UNIVERSITATIS OULUENSIS



ISBN 978-951-42-9544-7 (Paperback)
ISBN 978-951-42-9545-4 (PDF)
ISSN 0355-3213 (Print)
ISSN 1796-2226 (Online)

UNIVERSITY of OULU
OULUN YLIOPISTO